

Super-Linear: A Lightweight Pretrained Mixture of Linear Experts for Time Series Forecasting

Liran Nochumsohn¹ Raz Marshanski¹ Hedi Zisling¹ Omri Azencot¹

Abstract

Time series forecasting (TSF) is critical in domains like energy, finance, healthcare, and logistics, requiring models that generalize across diverse datasets. Large pre-trained models such as Chronos and Time-MoE show strong zero-shot (ZS) performance but suffer from high computational costs. In this work, We introduce Super-Linear, a lightweight and scalable mixture-of-experts (MoE) model for general forecasting. It replaces deep architectures with simple frequency-specialized linear experts, trained on resampled data across multiple frequency regimes. A lightweight spectral gating mechanism dynamically selects relevant experts, enabling efficient, accurate forecasting. Despite its simplicity, Super-Linear matches state-of-the-art performance while offering superior efficiency, robustness to various sampling rates, and enhanced interpretability. The implementation of Super-Linear is available at <https://github.com/azencot-group/SuperLinear>

1. Introduction

Time series forecasting plays a vital role in many high-impact domains, from optimizing energy grids and managing financial risk to supporting clinical decision-making and supply chain operations (Taylor & Letham, 2018; Salinas et al., 2020; Lim et al., 2021). As these systems increasingly rely on automated forecasting tools, the demand grows for models that can generalize across a wide range of temporal settings without manual tuning. However, many real-world scenarios involve small or heterogeneous datasets with unique periodic patterns, limited labels, and shifting dynamics (Norton et al., 2025). In such environments, training specialized models per dataset is computationally costly and often impractical. This motivates the need for *zero-shot forecasting* (ZSF), a setting in which a single model can

¹Faculty of Computer and Information Science, Ben-Gurion University. Correspondence to: Liran Nochumsohn <liran-noc@post.bgu.ac.il>.

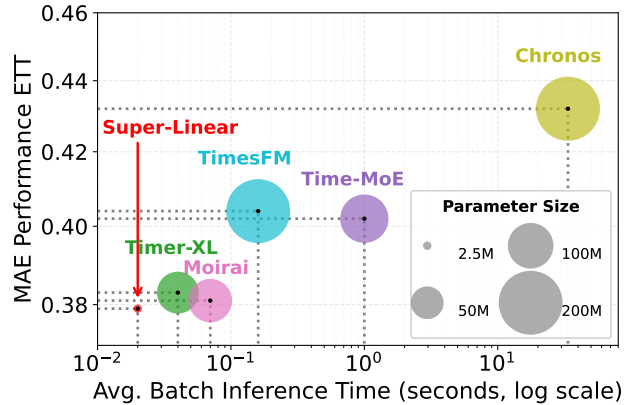


Figure 1. Performance versus inference time trade-off across different prominent pretrained TSF models.

generalize to entirely unseen datasets and domains without retraining or fine-tuning (Shi et al., 2024; Liu et al., 2024d;c; Das et al., 2024).

Recent work has made significant progress toward this goal. Large pretrained models such as Timer-XL, TimeMoE, and TimesFM (Liu et al., 2024c; Shi et al., 2024; Das et al., 2024) employ transformer-based backbones, input patching, and masked pretraining to achieve strong zero-shot performance across domains. However, these gains come at a high computational cost. For instance, TimeMoE was trained over several days using 28 A100-80GB GPUs, whereas Chronos can take over 10 seconds to generate an output for a batch size of 64 under certain configurations. See Fig. 1 for a general overview. Additionally, the complexity of these architectures also poses a challenge for interpretability, as their sophisticated designs make it difficult to understand or explain forecasting decisions. Developing models that combine strong generalization with greater transparency still remains a key challenge, which often hinders accessibility and practical deployment. As zero-shot forecasting becomes more practical, it is imperative to develop models that preserve strong generalization while dramatically reducing the computational and memory footprint.

Recent findings show that carefully constructed linear mod-

els can outperform deep transformer-based architectures across several TSF benchmarks (Zeng et al., 2023; Toner & Darlow, 2024; Ni et al., 2024; Nochumsohn et al., 202t). Consequently, linear forecasting models offer a promising foundation for efficient ZSF and *full-shot forecasting* (FSF). They are fast, lightweight, and well-aligned with the temporal structure of many natural sequences. However, a single linear model typically lacks the expressivity needed to generalize across diverse datasets (Nochumsohn et al., 202t). Capturing multiple overlapping frequencies with one parameter set induces what we term *frequency confusion*, where different temporal patterns compete for representation and degrade accuracy. This limitation is especially pronounced in zero-shot settings, where effective generalization requires both robustness to distribution shifts and adaptability to novel temporal patterns. Taken together, these challenges may explain why linear models remain relatively underexplored in zero-shot forecasting within pre-trained frameworks.

Toward bridging this gap, we introduce *Super-Linear*, a sparse mixture-of-experts (MoE) model that brings modularity and frequency-awareness to linear forecasting. Super-Linear comprises of linear heads most of which are trained to specialize in a particular frequency regime, using resampled data to ensure abundance and diversity of periodic signals. A lightweight, interpretable gating mechanism routes each input sequence to a subset of experts based on its spectral signature, dynamically assembling predictions without shared weights. Complementary experts and simple heuristics (e.g., naïve repeat, mean forecasting) provide further flexibility, allowing to recover accurate forecasts even in ambiguous or low-frequency settings.

Super-Linear combines the scalability and interpretability of linear models with the adaptability of MoE architectures. It is trained using standard procedures, requires no auxiliary loss functions or sophisticated optimization schemes, and runs efficiently on a single GPU. As we show in Fig. 1, Super-Linear achieves competitive performance relative to state-of-the-art zero-shot and full-shot forecasting models, while offering substantial improvements in inference speed and model size. We evaluate Super-Linear against leading state-of-the-art baselines across both zero-shot and full-shot regimes. Despite its small size, just 2.5 million parameters, Super-Linear achieves substantial improvements in zero-shot forecasting, reducing average MSE by up to 26.2% compared to prominent models like Chronos and TimesFM. It also outperforms Timer-XL in both MSE and MAE on more than twice as many benchmarks, while being only 3% of its size. In the GIFT-Eval benchmark (Aksu et al., 2024), Super-Linear achieves a competitive MASE score surpassing the performance of TSFM such as VisionTS, Moirai, and TTM (Chen et al., 2024; Woo et al., 2024; Ekambaram et al., 2024).

2. Related Work

Pre-trained Model in TSF. Recent advancements in pre-trained models for vision and text (Zhou et al., 2024) have accelerated the development of large time series foundation models for zero-shot, few-shot, and full-shot forecasting (Liang et al., 2024). Modern models like UniTime (Liu et al., 2024b), TEMPO (Cao et al., 2023), and GPT4TS (Zhou et al., 2023) adopted GPT-based architectures, inspiring works such as MOMENT (Goswami et al., 2024) and TimesFM (Das et al., 2024), which integrate transformers (Vaswani et al., 2017), input patching, and masked training to handle diverse inputs. Chronos (Ansari et al., 2024) leverages a T5-based architecture (Raffel et al., 2020) with discrete time tokenization, while Moirai (Woo et al., 2024) employs an encoder-only transformer with multi-patch size projections and binary attention biases for universal forecasting. Timer and Timer-XL (Liu et al., 2024d;c), as decoder-only generative models, use next-token prediction for flexible time series processing. Finally, Time-MoE (Shi et al., 2024), a decoder-only mixture-of-experts model, effectively scales parameters, enhancing accuracy and efficiency in forecasting.

Linear and sparse TSF Models. Before deep time series forecasting (TSF) gained traction, statistical and linear models such as ARIMA, Exponential Smoothing, and least squares regression (Shumway & Stoffer, 2000) dominated TSF. In recent years, MLP (multilayer perceptron) and transformer-based models initially outperformed these methods with models such as Informer, Autoformer, FEDformer, and N-HiTS (Zhou et al., 2021; Wu et al., 2021; Zhou et al., 2022; Challu et al., 2023), however, recent research has demonstrated that linear and sparse models such as DLinear and RLinear (Zeng et al., 2023; Toner & Darlow, 2024; Li et al., 2023) can be competitive or even superior. This has sparked interest in sparse and frequency-aware TSF models, including FITS and SparseTSF (Xu et al., 2023; Lin et al., 2024b), which leverage the frequency domain for improved forecasting. MTLLinear (Nochumsohn et al., 202t) addresses gradient conflicts with variate cross-correlation, enhancing robustness against transformers with linear models, while CycleNet (Lin et al., 2024a) employs a shallow MLP with learnable recurrent cycles to model periodic patterns efficiently. These approaches provide scalable and interpretable forecasting solutions, particularly for resource-constrained applications.

Mixture of Experts. Mixture of Experts (MoE) (Cai et al., 2024; Jacobs et al., 1991) enhances efficiency and scalability by dynamically selecting specialized sub-models for different tasks, reducing computational overhead while maintaining high performance. Although widely used in language models (Cai et al., 2024), MoE has been sparingly applied

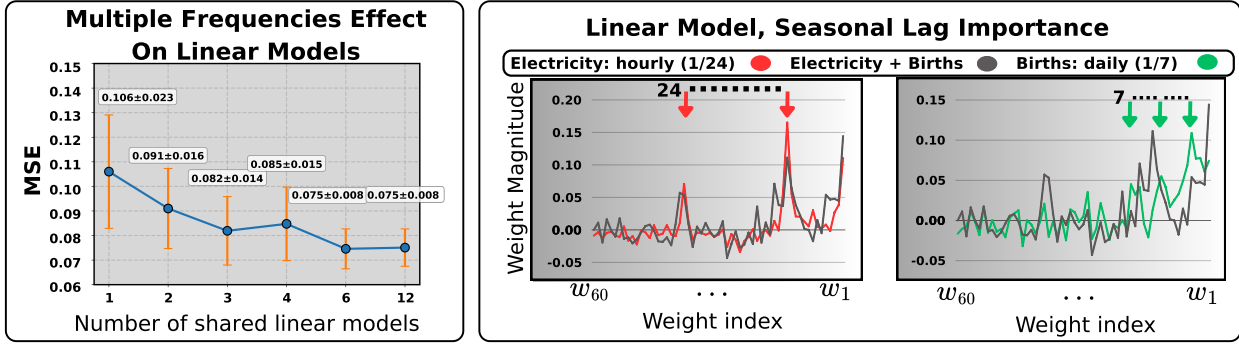


Figure 2. Left: Forecasting performance of linear models on 12 sine-wave datasets with varying frequencies and added random walk noise. Performance improves progressively with more experts. Right: Weight sensitivity to seasonal lags—training on datasets with different seasonality (e.g., Births vs. Electricity) leads to divergent weight structures, suboptimal when shared.

to time series forecasting, beginning with the Mixture of Experts Model (MEM) (Zeevi et al., 1996), which extends autoregressive models into a nonlinear universal approximator. Models such as FEDformer (Zhou et al., 2022) utilize MoE for different average pooling selection, while Moirai-MoE and Time-MoE (Woo et al., 2024; Shi et al., 2024), incorporate MoE within their designs. MoLE (Ni et al., 2024) introduces weighted linear experts for in-domain forecasting, and FreqMoE (Liu, 2025) processes distinct frequency bands for prediction. Our approach scales these ideas into a centralized, linear-enhanced pretrained model capable of handling diverse datasets while maintaining a sparse architectural design.

3. Super-Linear Mixture-of-Experts

Problem Formulation. Given a historical sequence of observations $X_{1:L} = [x_1, x_2, \dots, x_L]^T \in \mathbb{R}^L$, where L represents the number of lookback time steps, the goal in time series forecasting is to predict the future H steps $Y_{1:H} = X_{L+1:L+H} = [x_{L+1}, \dots, x_{L+H}]^T \in \mathbb{R}^H$. Super-Linear MoE leverages a modular architecture combining linear maps and expert gating mechanisms to enhance forecasting accuracy across diverse horizons with a single model, ranging from short-term (e.g., one step) to long-term (e.g., 720 steps and beyond). By dynamically selecting relevant experts based on input characteristics, the model adapts to varying frequencies and amplitudes. Furthermore, the integration of channel-wise independence ensures scalability to high-dimensional datasets, enabling Super-Linear to generalize effectively across multivariate forecasting tasks in real-world scenarios.

Motivation. Time series is naturally periodic, yet common methods, such as seasonal-trend decomposition or covariate timestamp embeddings (Ni et al., 2024), struggle with scalability and mixed-frequency signals (Theodosiou,

2011; Woo et al., 2022; Qin et al., 2024). Inspired by Fourier analysis (Shumway & Stoffer, 2000), we view a time series as a weighted sum of its dominant periodic components, with $\hat{\omega}_i$ denoting the characteristic frequencies and α_i are their amplitudes,

$$X \approx \alpha_1 X_{\hat{\omega}_1} + \alpha_2 X_{\hat{\omega}_2} + \dots + \alpha_k X_{\hat{\omega}_k}. \quad (1)$$

Linear forecasting models that take the form of an autoregressive process remain surprisingly effective (Zeng et al., 2023), and often learn to emphasize seasonal lags—e.g., daily or weekly offsets—when such structure exists. However, capturing multiple overlapping frequencies with a single weight vector is fundamentally limited. As different seasonalities compete, shared weights induce “frequency confusion” and degrade performance (see Fig. 2). To address this, we propose approximating forecasts using a mixture of frequency-specialized linear experts. Given input $X \in \mathbb{R}^{B \times T}$ and output $Y \in \mathbb{R}^{B \times H}$, where B is the batch size and T and H are the lookback and horizon, we have:

$$Y \approx \hat{Y} = \beta_1 F_{\hat{\omega}_1}(X) + \beta_2 F_{\hat{\omega}_2}(X) + \dots + \beta_k F_{\hat{\omega}_k}(X), \quad (2)$$

where each $F_{\hat{\omega}_i}$ models a specific frequency and β_i are data-dependent gating weights. This modular design mitigates interference, supports dynamic frequency selection, and improves generalization in complex forecasting tasks. A schematic illustration of our architecture is presented in Fig. 3.

Model Overview. Let $X \in \mathbb{R}^{B \times T}$ and $Y \in \mathbb{R}^{B \times H}$. Super-Linear produces a forecast $\hat{Y} \in \mathbb{R}^{B \times H}$ over a horizon of H steps. This forecast is computed as a weighted sum over N experts, each of which contributes a prediction $F_i(X) \in \mathbb{R}^{B \times H}$, modulated by a gating weight

$G_i(X) \in \mathbb{R}^B$:

$$\hat{Y} = \sum_{i=1}^N \text{diag}(G_i(X)) F_i(X), \quad (3)$$

where $\text{diag}(A)$ is the diagonal matrix in $\mathbb{R}^{B \times B}$ with the entries of $A \in \mathbb{R}^B$ on its main diagonal.

Linear Experts. Each expert F_i is a learnable or non-learnable linear model. The learnable experts consist of N_f frequency-specific modules and N_c complementary ones, implemented via RLinear—a linear layer combined with instance normalization using RevIN_{norm} (Toner & Darlow, 2024). This normalization mitigates distribution shifts by reapplying the input’s original scale after transformation. The output of each learnable expert is:

$$F_i(X) = \text{RevIN}^{-1}(\text{RevIN}(X)W_i + \text{rep}(b_i)), \quad (4)$$

where $W_i \in \mathbb{R}^{T \times H}$ and $b_i \in \mathbb{R}^H$ are trainable, and $\text{rep}(\cdot)$ repeats its input B times. Frequency experts are pre-trained for a specific $\hat{\omega}_i$ (App. C.3), covering diverse periodicities, while complementary experts are trained jointly to capture residual temporal signals. Two non-learnable experts, the *naïve* (last value) and *mean* (input average), serve as robust heuristics in low-frequency or short-sequence regimes. Including them improves performance across benchmarks (Tab. 3).

Gating Function. The weights $G_i(X)$ for combining expert outputs are derived through a sparse gating mechanism (Shazeer et al., 2017) that dynamically selects the most relevant experts based on the input’s spectral properties. Specifically, we compute a gating matrix $g(X) \in \mathbb{R}^{B \times N}$, where each entry reflects the affinity between the input and a given expert. These entries are computed using the normalized periodogram (Shumway & Stoffer, 2000; Schuster, 1898) of the zero-mean input. Formally,

$$g(X) = \frac{I(X - \bar{X})}{\|I(X - \bar{X})\|_1} W_g + b_g, \quad I(X - \bar{X}) = \left| \frac{\text{FFT}(X - \bar{X})}{\sqrt{2M}} \right|^2,$$

where $W_g \in \mathbb{R}^{M \times N}$ and $b_g \in \mathbb{R}^N$ are trainable parameters, FFT denotes the Fast Fourier Transform, and $2M$ is the number of spectral bins. Since the input is real-valued, the spectrum is symmetric and only the first M coefficients are retained. $I(X - \bar{X})$ is then normalized using the L_1 norm.

Sparse Gating. To encourage sparsity and specialization, only the top- k scoring experts are activated for each input. During training, we inject Gaussian noise $\mathcal{R}^{\text{noise}} \in \mathbb{R}^{B \times N}$ into the scores to promote exploration. The final gating weights, $G(X) \in \mathbb{R}^{B \times N}$, are computed using a softmax applied only over the top- k scores per column, i.e., TopK

eliminates the $B \times (N - k)$ smallest elements of $g(X) + \sigma \mathcal{R}^{\text{noise}}$ for $\sigma = 0.1$:

$$G(X) = \text{softmax}(\text{TopK}(g(X) + \sigma \mathcal{R}^{\text{noise}}, k)), \quad (5)$$

$$\text{TopK}_i(H, k) = \begin{cases} H_i, & \text{if } i \in \text{top-}k, \\ -\infty, & \text{otherwise.} \end{cases} \quad (6)$$

With H_i denoting the i -column of H . By incorporating spectral structure into the gating process and combining this with a diverse set of linear experts, Super-Linear is able to efficiently adapt to a variety of temporal phenomena, balancing model simplicity with strong empirical performance.

Training Mechanism. Super-Linear adopts a two-stage training framework, illustrated in Fig. 4: *Stage 1: Frequency expert pre-training.* Each expert is trained independently on data aligned with its designated fundamental frequency $\hat{\omega}_i$. To expose each expert to diverse temporal patterns, we apply extensive resampling augmentations using linear interpolation. Unlike prior work focused on dataset diversity, our emphasis is on *frequency abundance*, capturing a broad range of frequency instances rather than dataset heterogeneity. We thus select a subset of datasets from Monash (Godhewa et al., 2021) and PEMS (Liu et al., 2022) that provide sufficient sequence length for downsampling. Full details on dataset selection and resampling are provided in App. B.

Stage 2: MoE router training. After pre-training, we freeze the frequency expert weights and proceed to train the MoE router jointly with the complementary expert layers. During this stage, only the router (gating mechanism) and the lightweight complementary layers are updated. These complementary layers are specifically designed to refine predictions by capturing residual patterns not handled by the frequency experts. The router learns to dynamically select the most suitable expert based on the input signal characteristics. This stage supports either in-domain downstream tasks or pre-training on multi-frequency datasets to enable zero-shot generalization.

Varying Lookbacks Adaptability. Although Super-Linear is a linear forecaster with fixed lookback weights, it employs a heuristic to handle variable input lengths. If the lookback L_{input} is shorter than the training length ($L_{\text{train}} = 512$), the series is upsampled via linear interpolation; if longer, it is downsampled while preserving signal energy. After inference, outputs are rescaled to the original resolution. While this procedure implicitly alters signal frequencies, Super-Linear remains robust to such variations. More details and a detailed algorithm are provided in Appendix A.6.

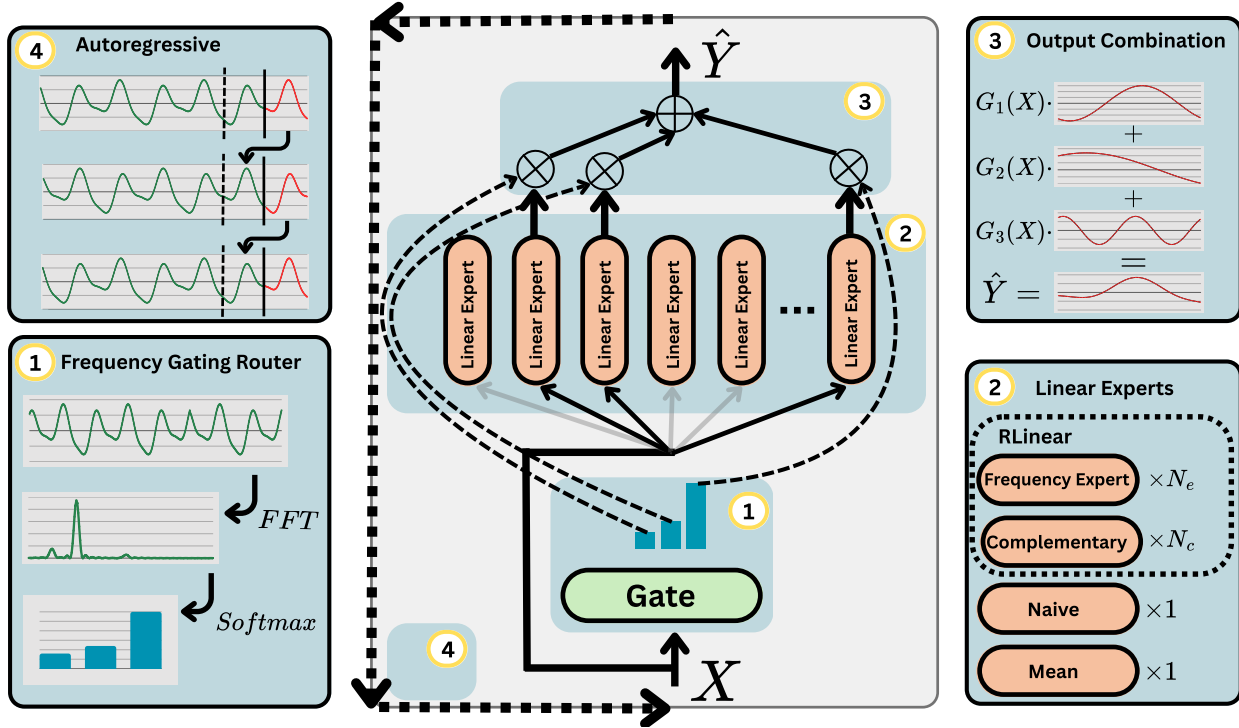


Figure 3. Super-Linear architecture overview. A frequency-aware gating router computes sparse scores from the input frequencies, dynamically selecting a subset of linear experts (1) including pre-trained frequency specialists, complementary modules, and heuristic naïve and mean baselines (2) whose predictions are combined to produce the final forecast (3).

4. Experiments

4.1. Experimental Details

Pre-training Datasets and Resampling. This work emphasizes frequency diversity over sheer dataset volume. For pre-training, we use two widely adopted sources: Monash (Godahewa et al., 2021) and PEMS (Liu et al., 2022). From Monash, only datasets with more than 5,000 samples are included, ensuring sufficient data for resampling. Resampling, both upsampling and downsampling, is performed on-the-fly during training via linear interpolation, eliminating the need to store multiple copies and saving space. We use the frequencies detailed in App. C.3. The same pre-training data is used across both training stages, as outlined in Sec. 3.

Training and Implementation. All Super-Linear models are trained on a single NVIDIA RTX3090 (24GB) using PyTorch (Paszke et al., 2019). In Stage 1, linear experts are trained independently and later combined into the Super-Linear architecture. We use the Adam optimizer with MSE loss and without auxiliary loss factors. For full-shot, the top-k experts are chosen via validation loss. All Super-Linear models use a lookback window of 512 and forecast a horizon of 96; longer horizons are predicted autoregressively. Full hyperparameters are detailed in App. E.

Baselines and Evaluations. We compare our method to top-performing models. For zero-shot, we benchmark against Timer-XL, ROSE, Time-MoE, Moirai, TimesFM, and Chronos (Liu et al., 2024c; Wang et al.; Shi et al., 2024; Woo et al., 2024; Das et al., 2024; Ansari et al., 2024), and focus mostly on models available on GitHub or Hugging Face. Evaluation follows the LTSF benchmark in both zero-shot and full-shot setups, using ETTm1, ETTm2, ETTh1, ETTh2, Electricity, Traffic, and Weather datasets (Liu et al., 2024c; Shi et al., 2024), including the GIFT-Eval benchmark (Aksu et al., 2024), which covers a wide range of dataset domains and sampling rates. The appendix includes additional evaluations such as full-shot (see Tab. 4), and extra model comparisons.

4.2. Main Results

LTSF: Zero-shot Forecasting and Model Size. In this section, we present the zero-shot (ZS) performance of Super-Linear in comparison to state-of-the-art (SOTA) models, given in Tab. 1. Despite having a relatively small number of parameters, Super-Linear achieves average mean squared error (MSE) reductions of **26.2%**, **14.2%**, **8.5%**, **7.1%**, and **6.3%** compared to Chronos, TimesFM, Moirai, Time-MoE Large, and Time-MoE Base, respectively. Additionally, Super-Linear outperforms Timer-XL by achieving 13

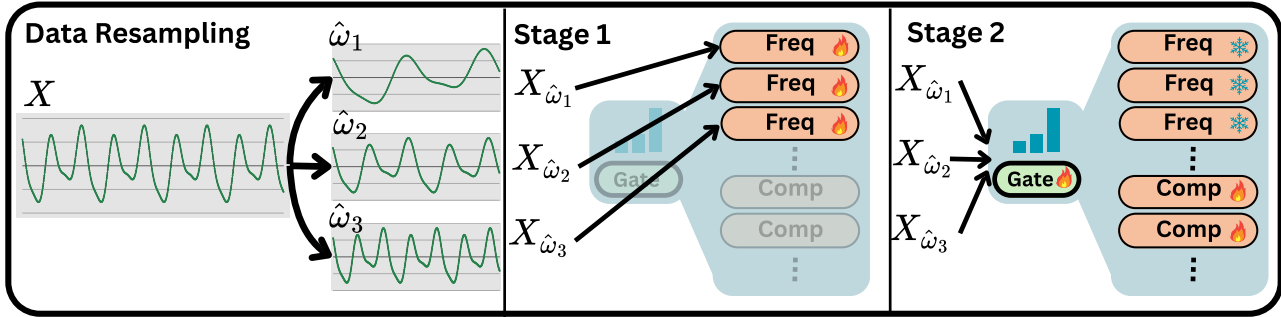


Figure 4. Super-Linear training framework. Data is resampled to enrich frequency diversity. Stage 1: Each expert is trained independently on a predefined frequency ω_i . Stage 2: The router and complementary layers are trained with frozen experts to enable dynamic expert selection.

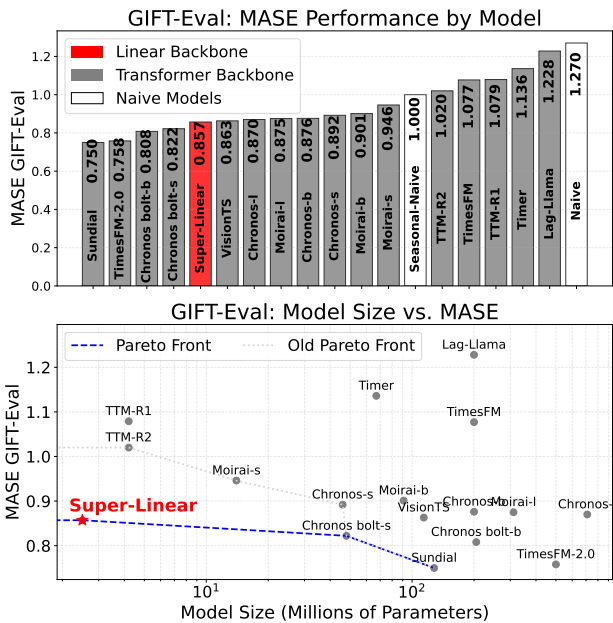


Figure 5. GIFT-Eval performance and parameter count of Super-Linear compared to prominent foundation models in TSF (Creation Date: 01/08/2025). The MASE score represents the geometric mean MASE across datasets, normalized by the seasonal-naive.

best scores in MSE and 16 best scores in mean absolute error (MAE), compared to Timer-XL’s 4 and 0 best scores. Remarkably, Super-Linear accomplishes this while being only 3% the size of Timer-XL, with only 2.5M parameters compared to 84M. To ensure fairness, we compare against models with similar lookback windows, excluding evaluations that rely on excessively long lookbacks, parameter search, or ensembles.

GIFT-Eval: Model Performance and Model Size. GIFT-Eval (Aksu et al., 2024) is a comprehensive benchmark

for time series forecasting, designed to fairly assess the zero-shot and universal forecasting capabilities of foundation models across diverse domains, frequencies, prediction lengths, and variates. We evaluate Super-Linear against state-of-the-art models including Sundial, VisionTS (Liu et al., 2025; Chen et al., 2024), Chronos, and TimesFM (Ansari et al., 2024; Das et al., 2024) in Fig. 5. Despite having the smallest parameter count (2.5M), Super-Linear achieves competitive results, delivering a 16% MASE reduction over TTM, the next smallest model, while being competitive or surpassing larger Transformer-based models such as VisionTS, TimesFM, and Sundial. Note that the GIFT-Eval leaderboard is continuously updated, and our results reflect peer-reviewed models available at the time stated in Fig. 5.

Zero-Shot Generalization Across Varying Sampling Rates. Existing pre-trained models exhibit a strong reliance on hourly-sampled datasets, which comprise between 59.4% and 93.1% of their training data (Fig. 6). In contrast, Super-Linear promotes frequency diversity by training on a balanced set of predefined sampling rates using linear interpolation. To assess robustness to underrepresented frequencies, an area often overlooked in TSF, we evaluate performance across a range of resampled datasets (Tab. 2). Super-Linear achieves the best results in 9 out of 11 scenarios and demonstrates the most consistent performance overall, which we attribute to its frequency-aware training and linear expert design. To ensure fairness, we apply only upsampling (avoiding external data leakage) and follow the standard LTSF training, validation, and test protocol used for ETT and Electricity.

Method Ablation. Table 3 presents the ablation study, reporting average MSE and MAE on the LTSF benchmark and the geometric mean on GIFT-EVAL. The full Super-Linear model achieves the best overall performance. Removing long lookback resampling substantially reduces generaliza-

Table 1. Zero-shot forecasting results (MSE & MAE) and model size. A dash (–) indicates datasets included in the model’s pre-training or no reported results. **Red** and **blue** highlight the best and second-best results per row, respectively. Time-MoE results are from (Shi et al., 2024); others from (Liu et al., 2024c).

Dataset	Horizon	Super-Linear		Timer-XL		ROSE		Time-MoE _{base}		Time-MoE _{Large}		Moirai		TimesFM		Chronos	
		MSE	MAE	MSE	MAE	MSE	MAE	MSE	MAE	MSE	MAE	MSE	MAE	MSE	MAE	MSE	MAE
ETT _{h1}	96	0.369	0.392	0.369	0.391	0.382	0.408	0.357	0.381	0.350	0.382	0.376	0.392	0.414	0.404	0.440	0.393
	192	0.399	0.410	0.405	0.413	0.400	0.420	0.384	0.404	0.388	0.412	0.412	0.413	0.465	0.434	0.492	0.426
	336	0.416	0.421	0.418	0.423	0.404	0.426	0.411	0.434	0.411	0.430	0.433	0.428	0.503	0.456	0.550	0.462
	720	0.424	0.439	0.423	0.441	0.420	0.447	0.449	0.477	0.427	0.455	0.447	0.444	0.511	0.481	0.882	0.591
	Avg.	0.402	0.416	0.404	0.417	0.401	0.425	0.400	0.424	0.394	0.420	0.417	0.419	0.473	0.444	0.591	0.468
ETT _{h2}	96	0.279	0.342	0.283	0.342	0.298	0.362	0.305	0.359	0.302	0.354	0.294	0.330	0.315	0.349	0.308	0.343
	192	0.333	0.379	0.340	0.379	0.336	0.385	0.351	0.386	0.364	0.385	0.365	0.375	0.388	0.395	0.384	0.392
	336	0.354	0.398	0.366	0.400	0.353	0.399	0.391	0.418	0.417	0.425	0.376	0.390	0.422	0.427	0.429	0.430
	720	0.389	0.425	0.397	0.431	0.395	0.432	0.419	0.454	0.537	0.496	0.416	0.433	0.443	0.454	0.501	0.477
	Avg.	0.339	0.386	0.347	0.388	0.346	0.394	0.366	0.404	0.405	0.415	0.363	0.382	0.392	0.406	0.406	0.410
ETT _{m1}	96	0.317	0.352	0.317	0.356	0.512	0.460	0.338	0.368	0.309	0.357	0.363	0.356	0.361	0.370	0.454	0.408
	192	0.357	0.375	0.358	0.381	0.512	0.462	0.353	0.388	0.346	0.381	0.388	0.375	0.414	0.405	0.567	0.477
	336	0.393	0.395	0.386	0.401	0.523	0.470	0.381	0.413	0.373	0.408	0.416	0.392	0.445	0.429	0.662	0.525
	720	0.459	0.432	0.430	0.431	0.552	0.490	0.504	0.493	0.475	0.477	0.460	0.418	0.512	0.471	0.900	0.591
	Avg.	0.382	0.388	0.373	0.392	0.525	0.470	0.394	0.416	0.376	0.406	0.407	0.385	0.433	0.419	0.646	0.500
ETT _{m2}	96	0.179	0.265	0.189	0.277	0.224	0.309	0.201	0.291	0.197	0.286	0.205	0.273	0.202	0.270	0.199	0.274
	192	0.240	0.305	0.241	0.315	0.266	0.333	0.258	0.334	0.250	0.322	0.275	0.316	0.289	0.321	0.261	0.322
	336	0.293	0.339	0.286	0.348	0.310	0.358	0.324	0.373	0.337	0.375	0.329	0.350	0.360	0.366	0.326	0.366
	720	0.382	0.392	0.375	0.402	0.395	0.407	0.488	0.464	0.480	0.461	0.437	0.411	0.462	0.430	0.455	0.439
	Avg.	0.273	0.325	0.273	0.336	0.299	0.352	0.318	0.366	0.316	0.361	0.312	0.337	0.328	0.347	0.310	0.350
Electricity	96	0.141	0.239	0.141	0.237	0.209	0.307	-	-	-	-	0.160	0.250	-	-	0.154	0.231
	192	0.157	0.253	0.159	0.254	0.219	0.315	-	-	-	-	0.175	0.263	-	-	0.179	0.254
	336	0.175	0.270	0.177	0.272	0.236	0.330	-	-	-	-	0.187	0.277	-	-	0.214	0.284
	720	0.217	0.306	0.219	0.308	0.273	0.328	-	-	-	-	0.228	0.309	-	-	0.311	0.346
	Avg.	0.172	0.267	0.174	0.268	0.234	0.320	-	-	-	-	0.188	0.275	-	-	0.214	0.279
Traffic	96	0.414	0.296	-	-	0.572	0.407	-	-	-	-	-	-	-	-	0.562	0.378
	192	0.430	0.300	-	-	0.575	0.406	-	-	-	-	-	-	-	-	0.579	0.412
	336	0.449	0.309	-	-	0.588	0.411	-	-	-	-	-	-	-	-	0.594	0.420
	720	0.551	0.344	-	-	0.618	0.422	-	-	-	-	-	-	-	-	0.723	0.472
	Avg.	0.461	0.312	-	-	0.588	0.412	-	-	-	-	-	-	-	-	0.614	0.420
Weather	96	0.159	0.211	0.171	0.225	0.200	0.260	0.160	0.214	0.159	0.213	0.220	0.217	-	-	0.203	0.238
	192	0.207	0.254	0.221	0.271	0.239	0.288	0.210	0.260	0.215	0.266	0.271	0.259	-	-	0.256	0.290
	336	0.261	0.293	0.274	0.311	0.279	0.315	0.274	0.309	0.291	0.322	0.286	0.297	-	-	0.314	0.336
	720	0.333	0.341	0.356	0.370	0.340	0.357	0.418	0.405	0.415	0.400	0.373	0.354	-	-	0.397	0.396
	Avg.	0.240	0.275	0.256	0.294	0.264	0.305	0.266	0.297	0.270	0.300	0.288	0.282	-	-	0.292	0.315
1st Count		17	19	4	0	3	0	1	2	5	0	0	6	0	0	0	1
Model Size		2.5M		84M		7.4M		113M		453M		91M		200M		201M	

tion on GIFT-EVAL, though performance remains competitive with models such as TTM and TiMER. Excluding complementary experts produces minor degradations, while removing the mean and naive experts has a more pronounced negative impact on GIFT-EVAL. Replacing the two-stage training with a single-stage setup leads to the largest performance drop, underscoring the importance of the proposed training scheme. For the LTSF results, all experiments use a forecast horizon of 96, with a fixed lookback length of 512, making long lookback resampling inapplicable.

4.3. Expert Analysis

Model Interpretability. One of Super-Linear’s key strengths lies in its interpretability through expert selection. Unlike deep MoE models such as Time-MoE, where multi-layered complexity hinders transparent analysis, Super-Linear employs a single expert layer, enabling direct examination of the softmax outputs. In Fig. 7, we present the

learned expert distributions for ETT, Weather, and Electricity. For example, the Electricity dataset, which is sampled hourly, predominantly activates the 1/24 expert, corresponding to hour/day periodicity. The Weather dataset tends to favor the 1/144 expert (10 min/day), and also often selects the naive expert, likely indicating the presence of noise or low-frequency dynamics. These distributions expose clear links between sampling rates, seasonal patterns, and expert activation, offering valuable insights into Super-Linear’s decision-making behavior.

Top-k Experts Ablation. Another insightful analysis involves evaluating performance as a function of the top- k experts hyperparameter for the sparse MoE. We conduct experiments with varying $k \in \{3, 6, 9, 12, 15\}$, as shown in Fig. 8. A key feature of Super-Linear is its ability to adapt the expert selection at inference time by recalibrating the expert distribution for any chosen $k \leq N$. Namely, we can pretrain on one k and evaluate on another k . In this experi-

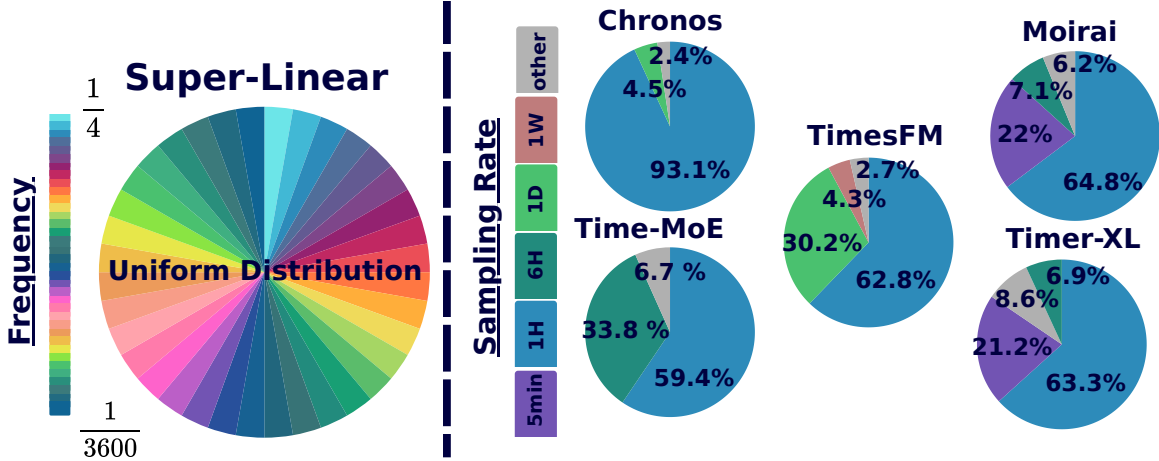


Figure 6. Dataset pre-training distribution for sampling rate or frequency. It is shown that other models rely heavily on hourly-sampled data. The frequencies for Super-Linear are given in App. 12.

Table 2. Zero-shot performance with varying sampling rates. The notations m, h and D represent per minute, hour, and day, respectively.

Model	ETT1-20m	ETT2-20m	ETT1-30m	ETT2-30m	ETT1-45m	ETT2-45m	ETT1-12h	ETT2-12h	ETT1-D	ETT2-D	Electricity-D
Super-Linear	0.371	0.170	0.408	0.189	0.422	0.207	0.665	0.509	0.746	0.586	0.644
Timer-XL	0.841	<u>0.199</u>	<u>0.437</u>	<u>0.208</u>	0.747	0.239	0.705	0.772	0.811	0.536	0.945
Time-MoE	0.663	0.223	0.449	0.222	0.575	0.268	<u>0.678</u>	0.542	<u>0.756</u>	<u>0.557</u>	0.751
Moirai	1.013	0.208	0.516	0.211	0.893	0.254	1.211	0.691	0.914	0.722	0.834
TimesFM	<u>0.514</u>	0.204	0.493	0.217	<u>0.552</u>	<u>0.236</u>	0.740	0.456	0.888	1.023	<u>0.719</u>
Chronos	0.764	0.212	0.585	0.211	0.738	0.250	1.032	<u>0.483</u>	0.945	0.678	0.751

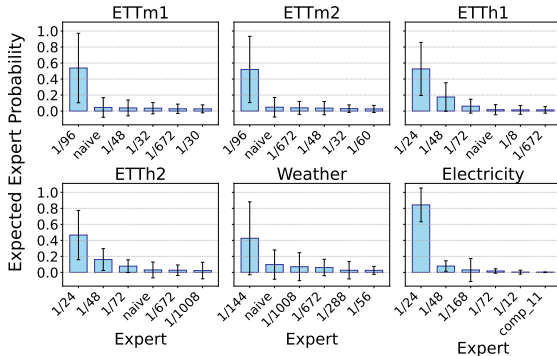


Figure 7. Top-k expert distribution for different datasets using the Super-Linear pretrained model.

ment, we assess the performance of a Super-Linear model pretrained with $k = 12$, comparing both inference-time adjustments (red curve) and retraining with different k values (blue curve). Results show dataset-dependent behavior, with a preference for the retrained setup for ETTh1, ETTm2, and Weather; however, adjusting the top- k at inference can be advantageous in some inference-time cases—for example, on ETTh1 and ETTm1, selecting $k = 3$ outperforms the original $k = 12$ configuration, despite the model being trained with $k = 12$. This highlights the practicality and adaptability of Super-Linear for zero-shot forecasting tasks.

Table 3. Ablation study on the full Super-Linear setup by systematically excluding each component of the framework: long lookback resampling, complementary experts, main and naive experts, and the two-stage training scheme.

Benchmark	full model	excl. resampling	excl. comp	excl. mean & Naive	excl. two-stage
LTSF-MSE	0.265	0.265	0.268	0.268	0.282
LTSF-MAE	0.3	0.3	0.304	0.304	0.315
G-EVAL-MASE	0.857	0.92	0.857	0.865	0.913

5. Theoretical Analysis

We provide a theoretical analysis of the gating mechanism through the lens of the *bias-complexity tradeoff* (Shalev-Shwartz & Ben-David, 2014), yielding bounds on the frequency approximation error. This framework helps assess the strengths and limitations of our frequency-specialized approach. Specifically, it decomposes the error of the ERM algorithm into a frequency-focused approximation error \mathcal{E}_{app} , representing bias from limited model capacity, and estimation error \mathcal{E}_{est} , arising from overfitting due to model complexity. By analyzing this tradeoff, we obtain theoretical insights into the robustness of the model and the gating mechanism. Assuming X and $Y(X)$ share the same periodicity, formally: $I^X = I^Y = I$, and for some $\gamma > 0$ we then get,

$$\begin{aligned} \|Y(X) - \hat{Y}(X)\| &= \mathcal{E}_{\text{app}} + \mathcal{E}_{\text{est}} \\ &\leq \sqrt{E_{\perp}} + \gamma \|X\|_2 \|\beta - G\|_1, \end{aligned} \quad (7)$$

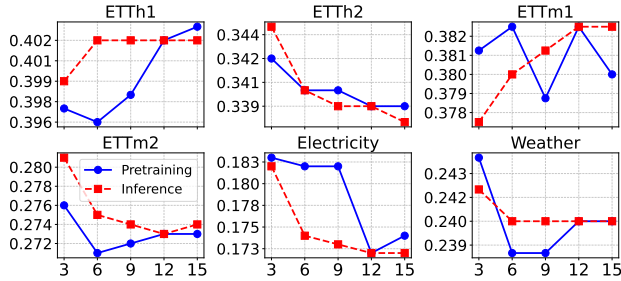


Figure 8. Top- k expert selection comparison. Performance across varying top- k expert settings. Blue and red vertical lines indicate the k values used during pretraining and inference, respectively.

- E_{\perp} bounds the (frequency)-approximation error: the signal energy outside the span of the N expert frequencies.
- The second term, which bounds the estimation error, penalises how far the learned gating G is from the optimal β . If training makes $\|\beta - G\|_1 \rightarrow 0$, the total error collapses to the intrinsic residual $\sqrt{E_{\perp}}$.

To ease notation, G , β , E_{\perp} represent $G(X)$, $\beta(X)$, and $E_{\perp}(X)$, respectively. Adding more frequency and complementary experts reduces approximation error but risks overfitting, while too few experts lead to underfitting, reflecting the bias–complexity trade-off (Shalev-Shwartz & Ben-David, 2014). Incorporating natural frequencies C.3 introduces a meaningful inductive bias, ensuring sufficient representative experts to cover diverse datasets while controlling complexity to prevent overfitting. In A.7, we provide the proof and provide an analysis with a stricter assumption on the shared periodicity.

6. Conclusion

Super-Linear is a sparse mixture-of-experts framework for zero-shot and full-shot time series forecasting that combines frequency-specialized linear experts with a spectral routing function to achieve efficient, accurate, and interpretable generalization across diverse benchmarks. While effective and scalable, its reliance on linear experts limits performance on highly nonlinear or chaotic series, suggesting future extensions with nonlinear or hybrid experts and more advanced routing strategies to enhance adaptability in complex settings.

References

Aksu, T., Woo, G., Liu, J., Liu, X., Liu, C., Savarese, S., Xiong, C., and Sahoo, D. Gift-eval: A benchmark for general time series forecasting model evaluation. *arXiv preprint arxiv:2410.10393*, 2024.

Ansari, A. F., Stella, L., Turkmen, C., Zhang, X., Mercado, P., Shen, H., Shchur, O., Rangapuram, S. S., Arango, S. P., Kapoor, S., et al. Chronos: Learning the language of time series. *arXiv preprint arXiv:2403.07815*, 2024.

Asuncion, A., Newman, D., et al. Uci machine learning repository, 2007.

Cai, W., Jiang, J., Wang, F., Tang, J., Kim, S., and Huang, J. A survey on mixture of experts. *arXiv preprint arXiv:2407.06204*, 2024.

Cao, D., Jia, F., Arik, S. O., Pfister, T., Zheng, Y., Ye, W., and Liu, Y. Tempo: Prompt-based generative pre-trained transformer for time series forecasting. *arXiv preprint arXiv:2310.04948*, 2023.

Challu, C., Olivares, K. G., Oreshkin, B. N., Ramirez, F. G., Canseco, M. M., and Dubrawski, A. N-HiTS: Neural Hierarchical Interpolation for Time Series Forecasting. In *Proceedings of the AAAI Conference on Artificial Intelligence*, 2023.

Chen, M., Shen, L., Li, Z., Wang, X. J., Sun, J., and Liu, C. Visionts: Visual masked autoencoders are free-lunch zero-shot time series forecasters, 2024. URL <https://arxiv.org/abs/2408.17253>.

Das, A., Kong, W., Sen, R., and Zhou, Y. A decoder-only foundation model for time-series forecasting. In *Forty-first International Conference on Machine Learning*, 2024.

Ekambaram, V., Jati, A., Dayama, P., Mukherjee, S., Nguyen, N., Gifford, W. M., Reddy, C., and Kalagnanam, J. Tiny time mixers (ttms): Fast pre-trained models for enhanced zero/few-shot forecasting of multivariate time series. *Advances in Neural Information Processing Systems*, 37:74147–74181, 2024.

Godahewa, R., Bergmeir, C., Webb, G. I., Hyndman, R. J., and Montero-Manso, P. Monash time series forecasting archive. In *Neural Information Processing Systems Track on Datasets and Benchmarks*, 2021.

Goswami, M., Szafer, K., Choudhry, A., Cai, Y., Li, S., and Dubrawski, A. Moment: A family of open time-series foundation models. *arXiv preprint arXiv:2402.03885*, 2024.

Jacobs, R. A., Jordan, M. I., Nowlan, S. J., and Hinton, G. E. Adaptive mixtures of local experts. *Neural computation*, 3(1):79–87, 1991.

Lai, G., Chang, W.-C., Yang, Y., and Liu, H. Modeling long-and short-term temporal patterns with deep neural networks. In *The 41st international ACM SIGIR conference on research & development in information retrieval*, pp. 95–104, 2018.

- Li, Z., Qi, S., Li, Y., and Xu, Z. Revisiting long-term time series forecasting: An investigation on linear mapping. *arXiv preprint arXiv:2305.10721*, 2023.
- Liang, Y., Wen, H., Nie, Y., Jiang, Y., Jin, M., Song, D., Pan, S., and Wen, Q. Foundation models for time series analysis: A tutorial and survey. In *Proceedings of the 30th ACM SIGKDD conference on knowledge discovery and data mining*, pp. 6555–6565, 2024.
- Lim, B., Arık, S. Ö., Loeff, N., and Pfister, T. Temporal fusion transformers for interpretable multi-horizon time series forecasting. *International Journal of Forecasting*, 37(4):1748–1764, 2021.
- Lin, S., Lin, W., Hu, X., Wu, W., Mo, R., and Zhong, H. Cyclenet: enhancing time series forecasting through modeling periodic patterns. *Advances in Neural Information Processing Systems*, 37:106315–106345, 2024a.
- Lin, S., Lin, W., Wu, W., Chen, H., and Yang, J. Sparsetsf: Modeling long-term time series forecasting with 1k parameters. *arXiv preprint arXiv:2405.00946*, 2024b.
- Liu, J., Liu, C., Woo, G., Wang, Y., Hooi, B., Xiong, C., and Sahoo, D. Unitst: Effectively modeling inter-series and intra-series dependencies for multivariate time series forecasting. *arXiv preprint arXiv:2406.04975*, 2024a.
- Liu, M., Zeng, A., Chen, M., Xu, Z., Lai, Q., Ma, L., and Xu, Q. Scinet: Time series modeling and forecasting with sample convolution and interaction. *Advances in Neural Information Processing Systems*, 35:5816–5828, 2022.
- Liu, X., Hu, J., Li, Y., Diao, S., Liang, Y., Hooi, B., and Zimmermann, R. Unitime: A language-empowered unified model for cross-domain time series forecasting. In *Proceedings of the ACM Web Conference 2024*, pp. 4095–4106, 2024b.
- Liu, Y., Hu, T., Zhang, H., Wu, H., Wang, S., Ma, L., and Long, M. itransformer: Inverted transformers are effective for time series forecasting. *arXiv preprint arXiv:2310.06625*, 2023.
- Liu, Y., Qin, G., Huang, X., Wang, J., and Long, M. Timer-xl: Long-context transformers for unified time series forecasting. *arXiv preprint arXiv:2410.04803*, 2024c.
- Liu, Y., Zhang, H., Li, C., Huang, X., Wang, J., and Long, M. Timer: Generative pre-trained transformers are large time series models. *arXiv preprint arXiv:2402.02368*, 2024d.
- Liu, Y., Qin, G., Shi, Z., Chen, Z., Yang, C., Huang, X., Wang, J., and Long, M. Sundial: A family of highly capable time series foundation models. *arXiv preprint arXiv:2502.00816*, 2025.
- Liu, Z. Freqmoe: Enhancing time series forecasting through frequency decomposition mixture of experts. *arXiv preprint arXiv:2501.15125*, 2025.
- Mancuso, P., Piccialli, V., and Sudoso, A. M. A machine learning approach for forecasting hierarchical time series. *Expert Systems with Applications*, 182:115102, 2021.
- Ni, R., Lin, Z., Wang, S., and Fanti, G. Mixture-of-linear-experts for long-term time series forecasting. In *International Conference on Artificial Intelligence and Statistics*, pp. 4672–4680. PMLR, 2024.
- Nie, Y., Nguyen, N. H., Sinthong, P., and Kalagnanam, J. A Time Series is Worth 64 Words: Long-term Forecasting with Transformers. In *The Eleventh International Conference on Learning Representations, ICLR, 2023*.
- Nochumsohn, L., Zisling, H., and Azencot, O. A multi-task learning approach to linear multivariate forecasting. In *International Conference on Artificial Intelligence and Statistics*. PMLR, 202t.
- Norton, D. A., Ott, E., Pomerance, A., Hunt, B., and Girvan, M. Tailored forecasting from short time series via meta-learning. *arXiv preprint arXiv:2501.16325*, 2025.
- Palaskar, S., Ekambaram, V., Jati, A., Gantayat, N., Saha, A., Nagar, S., Nguyen, N. H., Dayama, P., Sindhgatta, R., Mohapatra, P., et al. Automixer for improved multivariate time-series forecasting on business and it observability data. In *Proceedings of the AAAI conference on artificial intelligence*, pp. 22962–22968, 2024.
- Paszke, A., Gross, S., Massa, F., Lerer, A., Bradbury, J., Chanan, G., Killeen, T., Lin, Z., Gimelshein, N., Antiga, L., et al. PyTorch: An Imperative Style, High-Performance Deep Learning Library. *Advances in Neural Information Processing Systems*, 32, 2019.
- Qin, Z., Wei, B., Gao, C., and Ni, J. Kedformer: Knowledge extraction seasonal trend decomposition for long-term sequence prediction. *arXiv preprint arXiv:2412.05421*, 2024.
- Raffel, C., Shazeer, N., Roberts, A., Lee, K., Narang, S., Matena, M., Zhou, Y., Li, W., and Liu, P. J. Exploring the limits of transfer learning with a unified text-to-text transformer. *Journal of machine learning research*, 21(140):1–67, 2020.
- Salinas, D., Flunkert, V., Gasthaus, J., and Januschowski, T. DeepAR: Probabilistic forecasting with autoregressive recurrent networks. *International journal of forecasting*, 36(3):1181–1191, 2020.

- Schuster, A. On the investigation of hidden periodicities with application to a supposed 26 day period of meteorological phenomena. *Terrestrial Magnetism*, 3(1):13–41, 1898.
- Shalev-Shwartz, S. and Ben-David, S. *Understanding Machine Learning: From Theory to Algorithms*. Cambridge University Press, Cambridge, 1 edition, 2014.
- Shazeer, N., Mirhoseini, A., Maziarz, K., Davis, A., Le, Q., Hinton, G., and Dean, J. Outrageously large neural networks: The sparsely-gated mixture-of-experts layer. *arXiv preprint arXiv:1701.06538*, 2017.
- Shen, S., Van Beek, V., and Iosup, A. Statistical characterization of business-critical workloads hosted in cloud datacenters. In *2015 15th IEEE/ACM international symposium on cluster, cloud and grid computing*, pp. 465–474. IEEE, 2015.
- Shi, X., Wang, S., Nie, Y., Li, D., Ye, Z., Wen, Q., and Jin, M. Time-moe: Billion-scale time series foundation models with mixture of experts. *arXiv preprint arXiv:2409.16040*, 2024.
- Shumway, R. H. and Stoffer, D. S. *Time series analysis and its applications*, volume 3. Springer, 2000.
- Taylor, S. J. and Letham, B. Forecasting at scale. *The American Statistician*, 72(1):37–45, 2018.
- Theodosiou, M. Forecasting monthly and quarterly time series using stl decomposition. *International Journal of Forecasting*, 27(4):1178–1195, 2011.
- Toner, W. and Darlow, L. An analysis of linear time series forecasting models. *arXiv preprint arXiv:2403.14587*, 2024.
- Vaswani, A., Shazeer, N., Parmar, N., Uszkoreit, J., Jones, L., Gomez, A. N., Kaiser, Ł., and Polosukhin, I. Attention is all you need. *Advances in neural information processing systems*, 30, 2017.
- Wang, J., Jiang, J., Jiang, W., Han, C., and Zhao, W. X. Towards efficient and comprehensive urban spatial-temporal prediction: A unified library and performance benchmark. *arXiv e-prints*, pp. arXiv–2304, 2023.
- Wang, Y., Qiu, Y., Chen, P., Zhao, K., Shu, Y., Rao, Z., Pan, L., Yang, B., and Guo, C. Towards a general time series forecasting model with unified representation and adaptive transfer. In *Forty-second International Conference on Machine Learning*.
- Woo, G., Liu, C., Sahoo, D., Kumar, A., and Hoi, S. C. H. CoST: Contrastive learning of disentangled seasonal-trend representations for time series forecasting. In *The Tenth International Conference on Learning Representations, ICLR*. OpenReview.net, 2022.
- Woo, G., Liu, C., Kumar, A., Xiong, C., Savarese, S., and Sahoo, D. Unified training of universal time series forecasting transformers. In *Forty-first International Conference on Machine Learning, ICML*. OpenReview.net, 2024.
- Wu, H., Xu, J., Wang, J., and Long, M. Autoformer: Decomposition Transformers with Auto-Correlation for Long-Term Series Forecasting. *Advances in Neural Information Processing Systems*, 2021.
- Wu, H., Hu, T., Liu, Y., Zhou, H., Wang, J., and Long, M. Timesnet: Temporal 2d-variation modeling for general time series analysis. *arXiv preprint arXiv:2210.02186*, 2022.
- Xu, Z., Zeng, A., and Xu, Q. Fits: Modeling time series with 10k parameters. *arXiv preprint arXiv:2307.03756*, 2023.
- Zeevi, A., Meir, R., and Adler, R. Time series prediction using mixtures of experts. *Advances in neural information processing systems*, 9, 1996.
- Zeng, A., Chen, M., Zhang, L., and Xu, Q. Are transformers effective for time series forecasting? In *Proceedings of the AAAI conference on artificial intelligence*, pp. 11121–11128, 2023.
- Zhou, C., Li, Q., Li, C., Yu, J., Liu, Y., Wang, G., Zhang, K., Ji, C., Yan, Q., He, L., et al. A comprehensive survey on pretrained foundation models: A history from bert to chatgpt. *International Journal of Machine Learning and Cybernetics*, pp. 1–65, 2024.
- Zhou, H., Zhang, S., Peng, J., Zhang, S., Li, J., Xiong, H., and Zhang, W. Informer: Beyond Efficient Transformer for Long Sequence Time-Series Forecasting. In *Proceedings of the AAAI conference on artificial intelligence*, 2021.
- Zhou, T., Ma, Z., Wen, Q., Wang, X., Sun, L., and Jin, R. FEDformer: Frequency Enhanced Decomposed Transformer for Long-term Series Forecasting. In *International Conference on Machine Learning*. PMLR, 2022.
- Zhou, T., Niu, P., Sun, L., Jin, R., et al. One fits all: Power general time series analysis by pretrained lm. *Advances in neural information processing systems*, 36:43322–43355, 2023.

This appendix provides comprehensive supplementary material to support the main findings of our work. We present additional experimental results, ablation studies, theoretical analyses, and detailed descriptions of datasets and benchmark models. Section A covers full-shot and zero-shot forecasting results, including extensive comparisons with state-of-the-art baselines and ablation studies on model components and input lookback lengths. Section B offers a theoretical analysis of the Super-Linear model’s error decomposition. Section C details the datasets used for both pre-training and evaluation, while Section D describes the benchmark models considered in our comparisons. Finally, we provide further insights into the frequency expert weights and hyperparameter configurations used in our experiments.

A. Supplementary Experiments and Results

A.1. Full-Shot Forecasting

Full-Shot Forecasting. For full-shot, we evaluate against Timer-XL, UniTST, CycleNet, iTransformer, PatchTST, GPT4TS, TimesNet, and Autoformer (Liu et al., 2024c;a; Lin et al., 2024a; Liu et al., 2023; Nie et al., 2023; Zhou et al., 2023; Wu et al., 2022; 2021). Comparisons to additional MoE-based models are given in App. A.1. We evaluate Super-Linear against leading in-domain TSF models, with detailed results provided in Tab. 4. Results for CycleNet, GPT4TS, and PatchTST are drawn from their original papers, while others follow the evaluation setup of (Liu et al., 2024c). All baselines are assessed using comparable lookback windows: $L = 512$ for PatchTST and GPT4TS, $L = 720$ for CycleNet, and $L = 672$ for the remaining models. Super-Linear uses a fixed lookback of $L = 512$ and selects the best-performing model based on validation MSE across top- k experts, where $k \in 6, 8, 10, 12, 20$, with all other hyperparameters unchanged. It achieves the best MSE and MAE in **15** and **16** benchmarks, respectively—outperforming all competitors. On average, Super-Linear yields a **2.5%** and **3.9%** reduction in MSE compared to Timer-XL and CycleNet, respectively. Notably, it requires only a single training per dataset, with longer horizons handled autoregressively. Further, Stage 2 is repeated across three random seeds while training only on the target dataset and not on the pre-trained data.

Table 4. Full-shot (in-domain) forecasting results. **Red** and **blue** highlight the best and second-best results per row, respectively. Super-Linear utilizes a lookback of 512, the remaining models utilize a comparable lookback, equal to or greater than 512.

Dataset	Horizon	Super-Linear		Timer-XL		CycleNet		UniTST		iTransformer		PatchTST		GPT4TS		TimesNet		Autoformer	
		MSE	MAE	MSE	MAE	MSE	MAE	MSE	MAE	MSE	MAE	MSE	MAE	MSE	MAE	MSE	MAE	MSE	MAE
ETT1	96	0.364	0.392	0.364	0.397	0.385	0.412	0.379	0.415	0.387	0.418	0.370	0.400	0.376	0.397	0.452	0.463	0.467	0.499
	192	0.396	0.412	0.405	0.424	0.424	0.438	0.415	0.438	0.416	0.437	0.413	0.429	0.416	0.418	0.474	0.477	0.492	0.523
	336	0.417	0.426	0.427	0.439	0.460	0.463	0.440	0.454	0.434	0.450	0.422	0.440	0.442	0.433	0.493	0.489	0.519	0.531
	720	0.431	0.452	0.439	0.459	0.486	0.487	0.482	0.482	0.447	0.473	0.477	0.468	0.477	0.456	0.560	0.534	0.589	0.560
	Avg.	0.402	0.420	0.409	0.430	0.439	0.450	0.429	0.447	0.421	0.444	0.413	0.434	0.428	0.426	0.495	0.491	0.517	0.528
ETT2	96	0.272	0.335	0.277	0.343	0.293	0.352	0.343	0.398	0.297	0.349	0.274	0.337	0.285	0.342	0.340	0.374	0.358	0.397
	192	0.340	0.378	0.348	0.391	0.359	0.395	0.376	0.420	0.380	0.400	0.341	0.382	0.354	0.389	0.402	0.414	0.435	0.451
	336	0.369	0.405	0.375	0.418	0.392	0.423	0.399	0.435	0.428	0.432	0.329	0.384	0.373	0.407	0.452	0.452	0.454	0.475
	720	0.404	0.436	0.409	0.458	0.425	0.451	0.419	0.457	0.427	0.445	0.379	0.422	0.406	0.441	0.462	0.468	0.479	0.492
	Avg.	0.346	0.388	0.352	0.402	0.367	0.405	0.384	0.428	0.383	0.406	0.331	0.381	0.355	0.395	0.414	0.427	0.432	0.454
ETTm1	96	0.292	0.339	0.290	0.341	0.301	0.357	0.289	0.348	0.311	0.365	0.293	0.346	0.292	0.346	0.338	0.375	0.466	0.466
	192	0.332	0.364	0.337	0.369	0.341	0.377	0.332	0.375	0.353	0.390	0.333	0.370	0.332	0.372	0.371	0.387	0.504	0.496
	336	0.365	0.385	0.374	0.392	0.376	0.396	0.365	0.397	0.387	0.411	0.369	0.392	0.366	0.394	0.410	0.411	0.574	0.530
	720	0.425	0.423	0.437	0.428	0.431	0.425	0.421	0.431	0.452	0.445	0.416	0.420	0.417	0.421	0.478	0.450	0.596	0.558
	Avg.	0.354	0.378	0.360	0.382	0.362	0.389	0.352	0.388	0.376	0.403	0.353	0.382	0.352	0.383	0.399	0.406	0.535	0.512
ETTm2	96	0.164	0.250	0.175	0.257	0.176	0.265	0.171	0.260	0.183	0.272	0.166	0.256	0.173	0.262	0.187	0.267	0.255	0.339
	192	0.221	0.289	0.242	0.301	0.231	0.305	0.228	0.230	0.250	0.315	0.223	0.296	0.229	0.301	0.249	0.309	0.279	0.335
	336	0.272	0.324	0.293	0.337	0.282	0.338	0.282	0.336	0.311	0.356	0.274	0.329	0.286	0.341	0.321	0.351	0.331	0.374
	720	0.364	0.379	0.376	0.390	0.361	0.388	0.380	0.398	0.417	0.419	0.362	0.385	0.378	0.401	0.497	0.403	0.413	0.450
	Avg.	0.255	0.310	0.271	0.321	0.262	0.324	0.265	0.306	0.290	0.340	0.256	0.316	0.266	0.326	0.314	0.332	0.320	0.374
Electricity	96	0.131	0.225	0.127	0.219	0.127	0.223	0.130	0.225	0.133	0.229	0.132	0.232	0.139	0.238	0.184	0.288	0.256	0.357
	192	0.147	0.240	0.145	0.236	0.144	0.239	0.150	0.244	0.158	0.258	0.151	0.250	0.153	0.251	0.192	0.295	0.291	0.376
	336	0.164	0.258	0.159	0.252	0.159	0.255	0.166	0.262	0.168	0.262	0.171	0.272	0.169	0.266	0.200	0.303	0.290	0.379
	720	0.206	0.293	0.187	0.277	0.196	0.290	0.206	0.297	0.205	0.294	0.222	0.318	0.206	0.297	0.228	0.325	0.320	0.403
	Avg.	0.162	0.254	0.155	0.246	0.157	0.252	0.163	0.257	0.166	0.261	0.169	0.268	0.167	0.263	0.201	0.303	0.289	0.379
Weather	96	0.146	0.195	0.157	0.205	0.149	0.203	0.152	0.206	0.174	0.225	0.149	0.198	0.162	0.212	0.169	0.228	0.355	0.409
	192	0.189	0.237	0.206	0.250	0.192	0.244	0.198	0.249	0.227	0.268	0.194	0.241	0.204	0.248	0.222	0.269	0.421	0.450
	336	0.238	0.277	0.259	0.291	0.242	0.283	0.251	0.291	0.290	0.309	0.245	0.282	0.254	0.286	0.290	0.310	0.452	0.465
	720	0.312	0.328	0.337	0.344	0.312	0.333	0.322	0.340	0.374	0.360	0.314	0.334	0.326	0.337	0.376	0.364	0.513	0.496
	Avg.	0.221	0.259	0.240	0.272	0.224	0.266	0.231	0.272	0.266	0.290	0.225	0.264	0.236	0.271	0.264	0.293	0.435	0.455
1st Count		15	16	4	4	4	0	3	1	0	0	3	3	0	0	0	0	0	0

Table 5. Super-Linear full-shot comparison to Linear and MoE based models. All models utilize a lookback of 512.

Dataset	Horizon	Super-Linear		FreqMoE		MTLinear		MoLE		DLinear	
		MSE	MAE	MSE	MAE	MSE	MAE	MSE	MAE	MSE	MAE
ETTh1	96	0.364	0.392	0.690	0.568	0.411	0.430	0.379	0.406	0.371	0.399
	192	0.396	0.412	0.713	0.584	0.444	0.453	0.410	0.425	0.409	0.425
	336	0.417	0.426	0.717	0.595	0.458	0.458	0.432	0.439	0.438	0.444
	720	0.431	0.452	0.788	0.650	0.475	0.484	0.464	0.474	0.480	0.497
	Avg.	0.402	0.420	0.727	0.599	0.447	0.456	0.421	0.436	0.424	0.441
ETTh2	96	0.272	0.335	0.376	0.426	0.298	0.360	0.274	0.341	0.300	0.366
	192	0.340	0.378	0.401	0.441	0.358	0.399	0.325	0.377	0.386	0.419
	336	0.369	0.405	0.412	0.449	0.380	0.418	0.353	0.401	0.490	0.486
	720	0.404	0.436	0.469	0.484	0.401	0.438	0.393	0.431	0.784	0.629
	Avg.	0.346	0.388	0.414	0.450	0.359	0.404	0.336	0.388	0.490	0.475
ETTh1	96	0.292	0.339	0.500	0.462	0.310	0.354	0.306	0.352	0.308	0.351
	192	0.332	0.364	0.655	0.541	0.350	0.377	0.347	0.374	0.340	0.370
	336	0.365	0.385	0.652	0.542	0.382	0.395	0.377	0.391	0.373	0.393
	720	0.425	0.423	0.654	0.549	0.440	0.427	0.435	0.422	0.428	0.425
	Avg.	0.354	0.378	0.615	0.524	0.370	0.388	0.366	0.385	0.362	0.385
ETTh2	96	0.164	0.250	0.272	0.349	0.172	0.261	0.169	0.257	0.179	0.274
	192	0.221	0.289	0.314	0.372	0.227	0.298	0.227	0.297	0.253	0.332
	336	0.272	0.324	0.348	0.389	0.284	0.335	0.299	0.340	0.309	0.369
	720	0.364	0.379	0.439	0.442	0.373	0.392	0.380	0.393	0.398	0.419
	Avg.	0.255	0.310	0.343	0.388	0.264	0.322	0.269	0.322	0.285	0.349
Electricity	96	0.131	0.225	0.537	0.543	0.140	0.238	0.144	0.241	0.140	0.239
	192	0.147	0.240	0.532	0.538	0.169	0.272	0.159	0.257	0.156	0.257
	336	0.164	0.258	0.573	0.566	0.186	0.287	0.182	0.276	0.169	0.271
	720	0.206	0.293	0.520	0.529	0.224	0.318	0.200	0.287	0.206	0.306
	Avg.	0.162	0.254	0.540	0.544	0.180	0.279	0.171	0.265	0.168	0.268
Weather	96	0.146	0.195	0.191	0.244	0.148	0.201	0.221	0.218	0.173	0.232
	192	0.189	0.237	0.262	0.306	0.195	0.244	0.188	0.236	0.216	0.272
	336	0.238	0.277	0.299	0.331	0.245	0.282	0.240	0.276	0.259	0.307
	720	0.312	0.328	0.366	0.380	0.315	0.333	0.313	0.330	0.321	0.359
	Avg.	0.221	0.259	0.279	0.315	0.226	0.265	0.240	0.265	0.242	0.292
1st Count.		19	17	0	0	0	0	5	6	0	0

A.2. MoE and Linear Model Full-Shot Comparison

In this section, we compare the full-shot forecasting results presented in Table 4 with both traditional linear models—DLinear and MTLLinear (Zeng et al., 2023; Nochumsohn et al., 202t)—and Mixture-of-Experts (MoE)-based models, including FreqMoE and MoLE (Liu, 2025; Ni et al., 2024). These comparisons highlight the performance gains introduced by our proposed model, Super-Linear, in a full-data setting. As shown in Table 5, Super-Linear consistently outperforms the baselines, achieving the lowest Mean Squared Error (MSE) on 19 out of 24 benchmarks and the lowest Mean Absolute Error (MAE) on 17 out of 24. These results underscore the effectiveness of combining a mixture of pre-trained frequency experts and non-pretrained trainable experts for time series forecasting.

Setup. All evaluations are averaged over three runs with different random seeds and use a lookback window of 512 time steps. For fairness, we reimplement and reproduce results for FreqMoE, MTLLinear, MoLE, and DLinear using the same lookback length. A grid search is conducted over learning rates 0.01, 0.005, 0.001, 0.05, selecting the best configuration based on validation loss. For MTLLinear, we adopt the learning rate of 0.01 as recommended by the original authors.

A.3. Super-Linear comprehensive ZS Comparison to TTM

LTSF : In this section, we present a detailed comparison with the TTM model. Since the original work does not report MAE results, we provide an MSE-only comparison. We evaluate Super-Linear against both the TTM-Q results reported in the original paper and TTM-R2, which is available on Hugging Face. Across seven datasets, Super-Linear achieves superior performance in six cases on average as presented in Table 6.

GIFT-Eval : As shown in Figure 5, Super-Linear achieves a substantial performance gain of up to **16%** over TTM-R2, with a MASE score of **0.857** compared to **1.020**. This highlights the robustness of Super-Linear across diverse domains and sampling rates.

Table 6. Super-Linear zero-shot comparison to TTM. All models utilize a lookback of 512.

Dataset	Horizon	Super-Linear	TTM	TTM-R2
ETTm1	96	0.317	0.413	0.415
	192	0.357	0.476	0.380
	336	0.393	0.553	0.402
	720	0.459	0.737	0.446
	Avg.	0.382	0.545	0.411
ETTm2	96	0.179	0.187	0.186
	192	0.240	0.261	0.246
	336	0.293	0.323	0.324
	720	0.410	0.436	0.406
	Avg.	0.280	0.302	0.290
ETTTh2	96	0.279	0.285	0.286
	192	0.333	0.341	0.346
	336	0.354	0.383	0.385
	720	0.382	0.441	0.419
	Avg.	0.337	0.362	0.359
ETTTh1	96	0.369	0.365	0.363
	192	0.399	0.393	0.387
	336	0.416	0.415	0.402
	720	0.424	0.538	0.475
	Avg.	0.402	0.428	0.407
Electricity	96	0.141	0.169	0.170
	192	0.157	0.196	0.194
	336	0.175	0.209	0.213
	720	0.217	0.264	0.260
	Avg.	0.172	0.209	0.209
Weather	96	0.159	0.154	0.152
	192	0.207	0.203	0.195
	336	0.261	0.256	0.256
	720	0.333	0.329	0.319
	Avg.	0.240	0.235	0.230
Traffic	96	0.414	0.518	0.509
	192	0.430	0.548	0.538
	336	0.449	0.550	0.571
	720	0.551	0.605	0.617
	Avg.	0.461	0.555	0.559

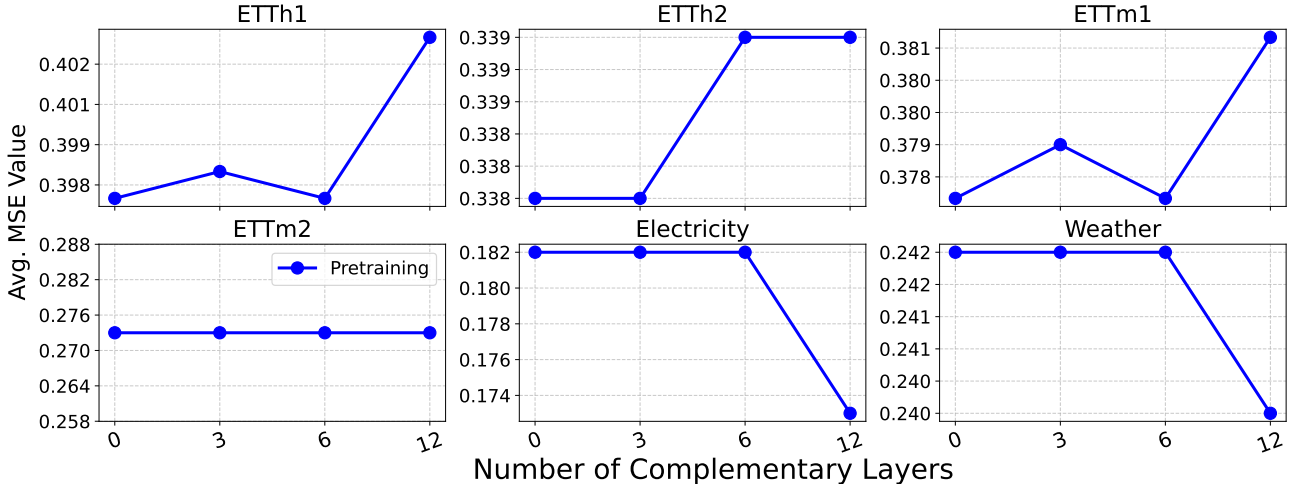


Figure 9. Complementary layer ablation for zero-shot evaluations across various datasets. The value 0 reflects Super-Linear with no complementary layers, whereas 12 represents Super-Linear with 12 complementary layers.

A.4. Complementary Experts Ablation

In this section, we evaluate the impact of the number of complementary layers used during pre-training across various datasets. The original pre-trained model, whose results are shown in Table 1, employs $N_c = 12$ complementary layers. Here, we explore a range of values for N_c to assess how this design choice affects performance. The results reveal that there is no universally optimal configuration: for datasets such as ETTh1, ETTh2, and ETTm1, introducing additional complementary layers can even degrade performance. In contrast, for datasets like Electricity and Weather, adding these layers yields significant improvements. This suggests that the effectiveness of complementary layers is dataset-dependent. One limitation of the current approach is the exclusive use of linear modules as complementary components—introducing non-linear transformations may offer further improvements and is a path for future exploration.

Experimental Setup. We follow the same training protocol described in Figure 4, and report average performance across four forecasting horizons: 96, 192, 336, and 720.

A.5. Full-Shot Results With Standard Deviation

Table 7 reports the standard deviation of the results presented in Table 4, calculated over three runs with different random seeds.

A.6. Full Ablation Results

In this section the full results of the LTSF ablation elements from Table 3.

A.7. Varying Input Lookbacks

$L_{\text{input}} < 512$. Although Super-Linear is a linear forecaster, it includes a simple built-in heuristic to handle variable lookback lengths. When the input lookback L_{input} is shorter than the training length ($L_{\text{train}} = 512$), the series is upsampled via linear interpolation to match 512. After inference, the output is downsampled back to the original resolution. This process implicitly modifies the signal’s frequency, but Super-Linear remains effective due to its robustness to frequency variations. The resampling factor is computed as:

$$\text{resample factor} = \left\lceil \frac{L_{\text{train}}}{L_{\text{input}}} \right\rceil$$

Table 7. Super-Linear full-shot with the standard deviation.

Dataset	Horizon	Super-Linear	
		MSE	MAE
ETTh1	96	0.364 ± 0.001	0.392 ± 0.001
	192	0.396 ± 0.001	0.412 ± 0.001
	336	0.417 ± 0.002	0.426 ± 0.001
	720	0.431 ± 0.002	0.452 ± 0.002
ETTh2	96	0.272 ± 0.001	0.335 ± 0.003
	192	0.340 ± 0.005	0.378 ± 0.004
	336	0.369 ± 0.010	0.405 ± 0.005
	720	0.404 ± 0.013	0.436 ± 0.011
ETTh1	96	0.292 ± 0.002	0.339 ± 0.001
	192	0.332 ± 0.001	0.364 ± 0.001
	336	0.365 ± 0.001	0.385 ± 0.002
	720	0.425 ± 0.001	0.423 ± 0.003
ETTh2	96	0.164 ± 0.001	0.250 ± 0.001
	192	0.221 ± 0.002	0.289 ± 0.001
	336	0.272 ± 0.003	0.324 ± 0.001
	720	0.364 ± 0.002	0.379 ± 0.001
Electricity	96	0.131 ± 0.000	0.225 ± 0.001
	192	0.147 ± 0.001	0.240 ± 0.000
	336	0.164 ± 0.000	0.258 ± 0.001
	720	0.206 ± 0.001	0.293 ± 0.001
Weather	96	0.146 ± 0.001	0.195 ± 0.001
	192	0.189 ± 0.000	0.237 ± 0.001
	336	0.238 ± 0.001	0.277 ± 0.001
	720	0.312 ± 0.001	0.328 ± 0.001

Table 8. Super-Linear full-shot comparison to Linear and MoE based models. All models utilize a lookback of 512.

Dataset	Full Model		excl. complimentary		excl. mean & naive		excl. two-stage	
	MSE	MAE	MSE	MAE	MSE	MAE	MSE	MAE
ETTh1	0.369	0.392	0.365	0.393	0.365	0.392	0.385	0.410
ETTh2	0.279	0.342	0.279	0.342	0.278	0.342	0.284	0.350
ETTh1	0.317	0.352	0.314	0.350	0.315	0.351	0.352	0.376
ETTh2	0.179	0.265	0.179	0.265	0.178	0.264	0.189	0.274
Electricity	0.141	0.239	0.151	0.249	0.150	0.248	0.154	0.255
Traffic	0.414	0.296	0.425	0.317	0.425	0.317	0.447	0.323
Weather	0.159	0.211	0.160	0.212	0.162	0.214	0.164	0.215

To revert the output, we interpolate with a factor of $\frac{1}{\text{resample factor}}$. This approach enables Super-Linear to effectively handle a range of input lengths. Examples below illustrate forecasting with lookbacks of 384, 256, and 128 on the Electricity and Weather datasets.

$L_{\text{input}} > 512$. The long lookback resample search algorithm adaptively downsamples time series by evaluating a set of candidate scales (default: [2, 4, 6]). For each sequence, it computes the power spectral density (PSD) to estimate signal energy, uses the expert distribution of Super-Linear to assess selection uncertainty, and applies linear interpolation for resampling. The objective is to minimize both energy loss and distributional entropy. To this end, we define a scoring function $score = entropy + \lambda \cdot penalty$, and select the resampling scale with the lowest score. A detailed description of the algorithm is provided in 1. Here is an overview of the flow of the algorithm:

- **Lines 1-3**, Compute the normalized periodogram I_{norm} , and the maximal scale factor s_{max} allowed such that the energy loss will not surpass $E_{max\ loss}$.
- **Lines 4-10**, create a dictionary $A_{penalty}$ that saves the estimated energy loss incurred by each scale parameter $s_i \in S$.
- **Lines 13-23**, Search for the best scale parameter that ensures minimal entropy score energy loss with the term $score = entropy(G(X_{interp})) + \lambda A_{penalty}[s]$.
- **Line 24** Finally, return the interpolated input X_{output} and the corresponding scale factor s_{output} , which will be used for resampling the output from Super-Linear to the original granularity.

In summary, the algorithm handles long-context inputs containing low-frequency components that may fall outside the range

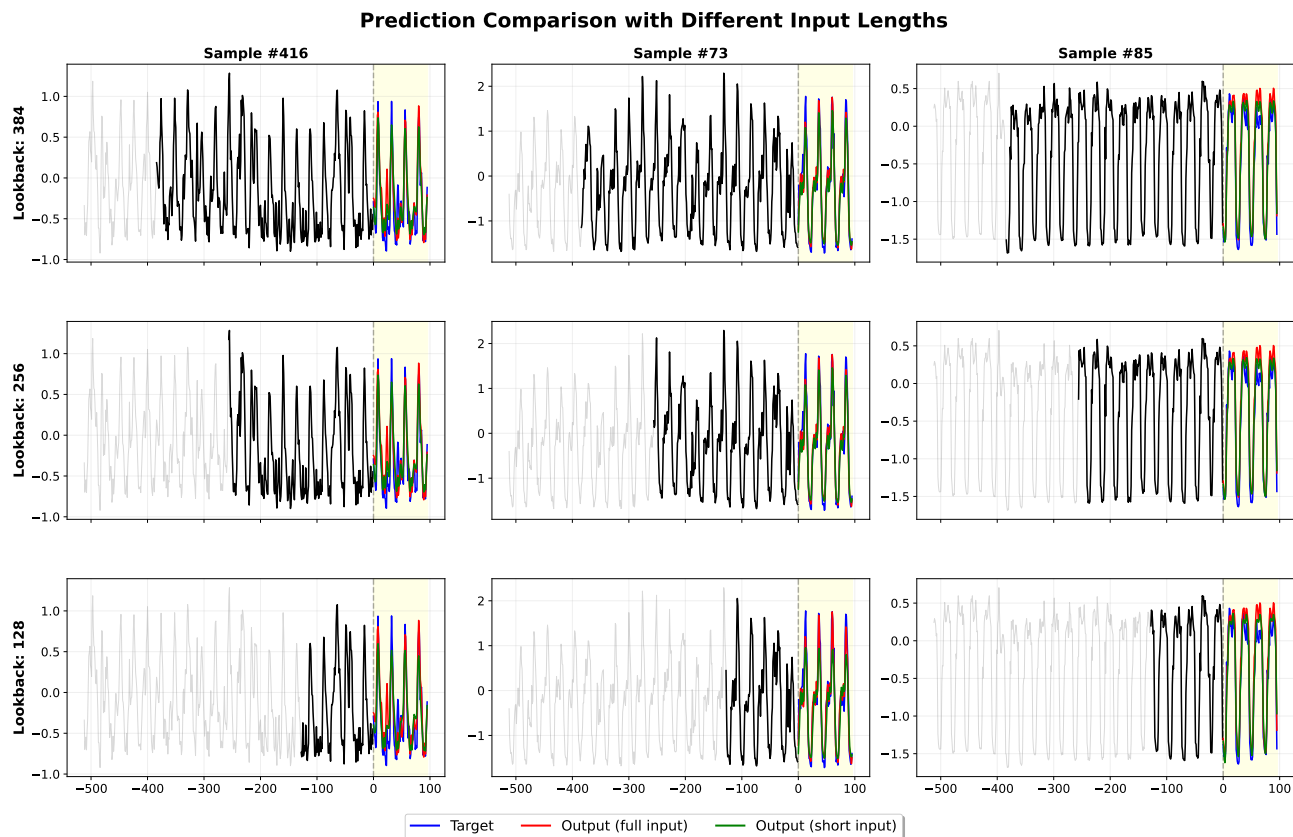


Figure 10. Super-Linear forecasting illustration with varying input lookbacks for the Electricity dataset.

of Super-Linear’s frequency experts. It selects an appropriate resampling factor that shifts the input frequencies into a space the model can represent, while preserving the signal’s energy to avoid information loss.

Algorithm 1 Long Lookback Resample Search Algorithm

- 1: **Input:** $X \in \mathbb{R}^L$, scales $S = \{s_1, s_2, \dots\}$, energy loss penalty scaler λ , a pre-trained Super-Linear model, and a parameter $E_{\max \text{ loss}}$ for the maximal energy loss constraint.
 - 2: $I_{\text{norm}} \leftarrow \frac{I(X-X)}{\|I(X-X)\|_1} \in \mathbb{R}^M$ (Periodogram normalization)
 - 3: $j^* \leftarrow \max\{j \mid E_j \leq 1 - E_{\max \text{ loss}}\}$ where $E_j = \sum_1^j I_{\text{norm}}^j$, and $E_M = 1$.
 - 4: $s_{\max} \leftarrow \lfloor \frac{\omega_{j^*}}{\omega_{\min}} \rfloor$ (ω_{\min} marks the highest frequency experts)
 - 5: $A_{\text{penalty}} \leftarrow \{\}$ (dictionary to track energy loss of each scale s)
 - 6: **for each** $s \in S, s > 1$ **do**
 - 7: $\omega_{\text{Nyq}} \leftarrow \frac{0.5}{s}$
 - 8: $I_s \leftarrow \{I_{\text{norm}}^j \mid \omega_j > \omega_{\text{Nyq}}\}$
 - 9: $E_{\text{lost}} \leftarrow \|I_s\|_1$
 - 10: $A_{\text{penalty}}[s] \leftarrow \frac{E_{\text{lost}}}{E_{\text{total}} + \varepsilon}$ where $\varepsilon \approx 10^{-10}$
 - 11: **end for**
 - 12: $X_{\text{output}} \leftarrow X$
 - 13: $s_{\text{output}} \leftarrow 1$
 - 14: $\text{score}_{\text{best}} \leftarrow \text{entropy}(G(X))$
 - 15: **for each** $s \in S, s > 1$ **do**
 - 16: $X_{\text{interp}} \leftarrow \text{interpolate}(X, \frac{1}{s}) \in \mathbb{R}^{L_{\text{interp}}}$
 - 17: **if** $L_{\text{train}} \leq L_{\text{interp}}$ **and** $s \leq s_{\max}$ **then**
 - 18: $\text{score} \leftarrow \text{entropy}(G(X_{\text{interp}})) + \lambda A_{\text{penalty}}[s]$
 - 19: **if** $\text{score} < \text{score}_{\text{best}}$ **then**
 - 20: $s_{\text{output}} \leftarrow s$
 - 21: $X_{\text{output}} \leftarrow X_{\text{interp}}$
 - 22: **end if**
 - 23: **end if**
 - 24: **end for**
 - 25: **Output:** $X_{\text{output}} \in \mathbb{R}^{L_{\text{interp}}}, s_{\text{output}}$
-

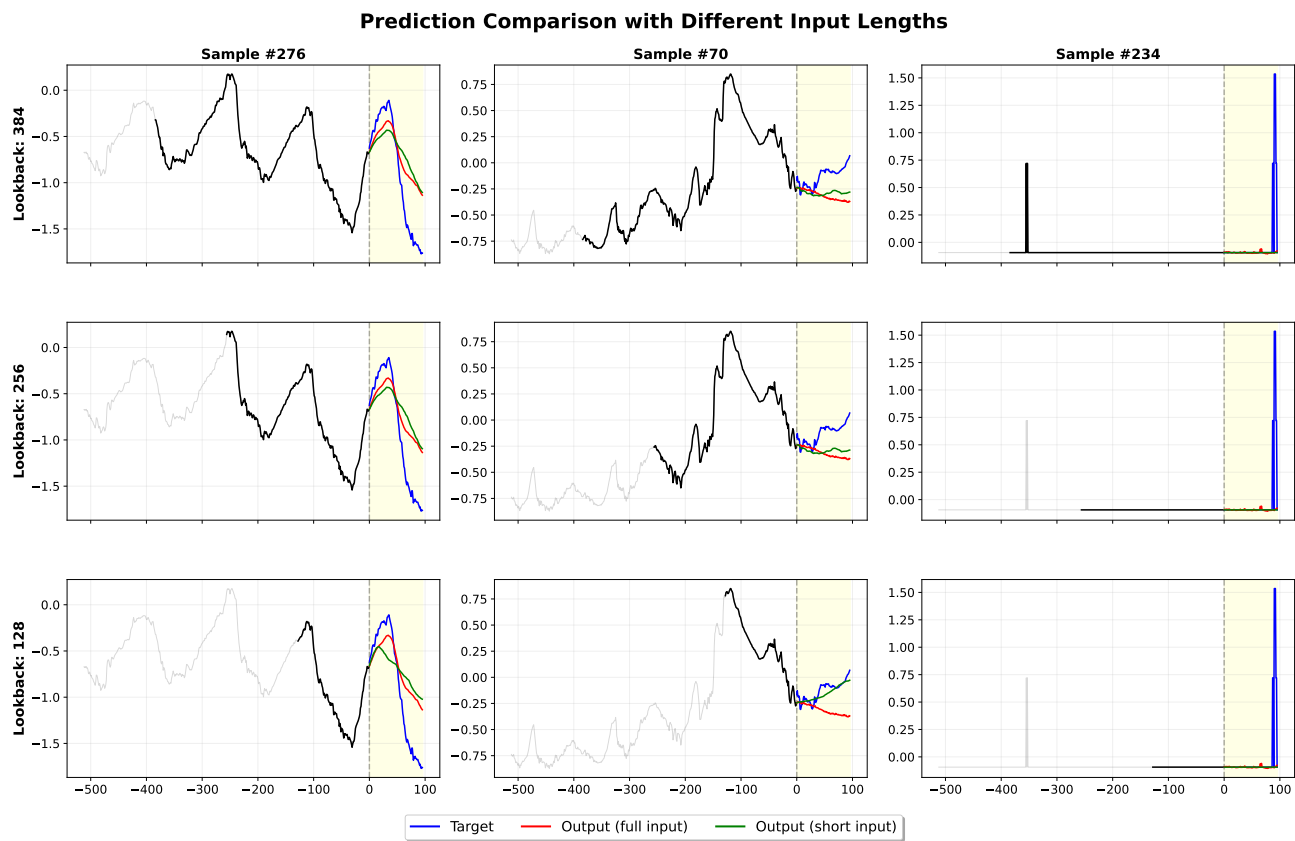


Figure 11. Super-Linear forecasting illustration with varying input lookbacks for the Weather dataset.

B. Theoretical Analysis

Following the *bias-complexity tradeoff* analysis (Shalev-Shwartz & Ben-David, 2014), we can decompose the error into the approximation error \mathcal{E}_{app} , and estimation error \mathcal{E}_{est} . The term \mathcal{E}_{app} represents the minimum achievable error by the Super-Linear predictor, whereas the term \mathcal{E}_{est} measures the difference between the approximation error and the error achieved by the ERM predictor with the given training data.

First by the triangle inequality:

$$\begin{aligned} \|Y(X) - \hat{Y}(X)\| &= \left\| Y(X) - \sum_{i=1}^N \bar{\beta}_i F_i(X) + \sum_{i=1}^N \bar{\beta}_i F_i(X) - \sum_{i=1}^N \bar{G}_i F_i(X) \right\| \\ &\leq \left\| Y(X) - \sum_{i=1}^N \bar{\beta}_i F_i(X) \right\| + \left\| \sum_{i=1}^N (\bar{\beta}_i - \bar{G}_i) F_i(X) \right\| \\ &= \mathcal{E}_{\text{app}} + \mathcal{E}_{\text{est}} \end{aligned}$$

1. (Frequency) Approximation term \mathcal{E}_{app} . Let $\mathcal{S} := \{\hat{\omega}_1, \dots, \hat{\omega}_N\}$ be the set of frequencies covered by the experts. Write the Fourier expansion of the (zero-mean) target as

$$Y(X) = \sum_m \hat{X}_m e^{2\pi i m \cdot / T}, \quad I_m = |\hat{X}_m|^2.$$

For now, let's assume that X and $Y(X)$, share the same periodicity, formally: $I_m^X = I_m^Y = I_m$. In the following section, we will remove this assumption.

Because each F_i reproduces its $\hat{\omega}_i \in \mathcal{S}$, the residual after projecting onto those frequencies is

$$\|Y(X) - R(X)\|_2^2 = \sum_{\omega_m \notin \mathcal{S}} I_m =: E_{\perp}(X).$$

Hence

$$\boxed{\mathcal{E}_{\text{app}} \leq \sqrt{E_{\perp}(X)}}.$$

2. Estimation term \mathcal{E}_{est} . Assume each expert output is bounded by the energy of its frequency, i.e.

$$\|F_i(X)\|_2 \leq \gamma \sqrt{I_i}, \quad \text{for some } \gamma > 0.$$

Using Cauchy-Schwarz and the fact that $\sum_i (\bar{\beta}_i - \bar{G}_i) = 0$ (both weight vectors sum to 1):

$$\begin{aligned} \mathcal{E}_{\text{est}} &= \left\| \sum_i (\bar{\beta}_i - \bar{G}_i) F_i(X) \right\|_2 \\ &\leq \left(\sum_i (\bar{\beta}_i - \bar{G}_i)^2 \right)^{1/2} \left(\sum_i \|F_i(X)\|_2^2 \right)^{1/2} \\ &\leq \gamma \|\beta - G\|_2 \left(\sum_i I_i \right)^{1/2} \\ &= \gamma \|\beta - G\|_2 \|X\|_2. \end{aligned}$$

Because $\|\cdot\|_2 \leq \|\cdot\|_1$ on probability simplices,

$$\boxed{\mathcal{E}_{\text{est}} \leq \gamma \|X\|_2 \|\beta - G\|_1}.$$

3. Combined bound. Putting the two pieces together,

$$\boxed{\|Y(X) - \hat{Y}(X)\| \leq \sqrt{E_{\perp}(X)} + \gamma \|X\|_2 \|\beta - G\|_1}.$$

Remarks.

- $E_{\perp}(X)$ bounds the *(frequency)-approximation error*: the signal energy outside the span of the N expert frequencies.
- The second term penalises how far the learned gating $G(X)$ is from the optimal $\beta(X)$. If training makes $\|\beta - G\|_1 \rightarrow 0$, the total error collapses to the intrinsic residual $\sqrt{E_{\perp}(X)}$.

To incorporate a stricter assumption on the shared periodicity. Specifically, we'll define δ_m as a frequency-dependent factor representing the relative difference in power at frequency ω_m . To model a measurable difference, we assume δ_m is small, i.e., $|\delta_m| \leq \epsilon, \forall m$ for some small $\epsilon > 0$, and δ_m can be positive or negative (indicating amplification or attenuation of power at specific frequencies). For simplicity, we can bound the difference across all frequencies.

$$I_m^Y = (1 + \delta_m)I_m^X, \quad \sum_{\omega_m \notin \mathcal{S}} I_m^X := E_{\perp}^X(X), \quad \sum_{\omega_m \notin \mathcal{S}} I_m^Y := E_{\perp}(X)$$

To bound this, we use the fact that $|\delta_m| \leq \epsilon$:

$$(1 + \delta_m)I_m^X \leq (1 + \epsilon)I_m^X$$

Hence,

$$\mathcal{E}_{\text{app}} \leq \sqrt{E_{\perp}} \leq \sqrt{1 + \epsilon} \sqrt{E_{\perp}^X(X)}$$

Table 9. Datasets used for pre-training.

Dataset	Source	Channels	Min/max channel length	Sampling rate	Frequency	Domain
London Smart Meters	(Godaheva et al., 2021)	5,560	288/39,648	30min	$\frac{1}{48}$	Energy
Aus. Electricity Demand	(Godaheva et al., 2021)	5	230,736/232,272	30min	$\frac{1}{48}$	Energy, Environmental
Wind Farms	(Godaheva et al., 2021)	339	6,345/527,040	minutely	$\frac{1}{1440}$	Energy
KDD Cup 2018	(Godaheva et al., 2021)	270	9,504/10,920	hourly	$\frac{1}{24}$	Nature, Environmental
Weather (Monash)	(Godaheva et al., 2021)	3,010	1,332/65,981	daily	$\frac{1}{7}$	Nature
Solar	(Godaheva et al., 2021)	137	52,560	10min	$\frac{1}{144}$	Nature
Sunspot	(Godaheva et al., 2021)	1	23,741	daily	$\frac{1}{27}$	Nature
Pedestrian	(Godaheva et al., 2021)	66	576/96424	hourly	$\frac{1}{24}$	Transport, Social
Us Births	(Godaheva et al., 2021)	1	7,305	daily	$\frac{1}{7}$	Nature
Saugeen River Flow	(Godaheva et al., 2021)	1	23,741	daily	$\frac{1}{365}$	Nature
Solar Power	(Godaheva et al., 2021)	1	7,397,222	4sec	$\frac{1}{21600}$	Energy
Wind Power	(Godaheva et al., 2021)	1	7,397,147	4sec	$\frac{1}{21600}$	Energy
PEMS03	(Liu et al., 2023)	358	25,887	5min	$\frac{1}{288}$	Transport
PEMS04	(Liu et al., 2023)	307	16,992	5min	$\frac{1}{288}$	Transport
PEMS07	(Liu et al., 2023)	883	28,224	5min	$\frac{1}{288}$	Transport
PEMS08	(Liu et al., 2023)	170	17,856	5min	$\frac{1}{288}$	Transport

Table 10. LTF benchmark Datasets used for evaluation in this work.

Dataset	Source	Channels	Min/max channel length	Sampling rate	Frequency	Domain	Usage
ETTh1	(Wu et al., 2021; Zhou et al., 2021)	7	17,420	hourly	-	Energy	Evaluation
ETTh2	(Wu et al., 2021; Zhou et al., 2021)	7	17,420	hourly	-	Energy	Evaluation
ETTh1	(Wu et al., 2021; Zhou et al., 2021)	7	69,680	15min	-	Energy	Evaluation
ETTh2	(Wu et al., 2021; Zhou et al., 2021)	7	69,680	15min	-	Energy	Evaluation
Electricity	(Wu et al., 2021; Zhou et al., 2021)	321	26,304	hourly	-	Energy	Evaluation
Traffic	(Wu et al., 2021; Zhou et al., 2021)	862	17,544	hourly	-	Transport, Environmental	Evaluation
Weather	(Wu et al., 2021; Zhou et al., 2021)	21	52,696	10min	-	Nature	Evaluation

C. Datasets

C.1. Pre-training Datasets

In this work, we pre-train Super-Linear using a subset of datasets from the Monash Time Series Repository (Godaheva et al., 2021) and the PEMS dataset (Liu et al., 2022), as part of the two-stage training process shown in Figure 4. Specifically, we select datasets with a minimum sequence length of 5,000 timesteps to enable sufficient downsampling. For upsampling, we cap the maximum resampling factor at $r_{\max} = 20$, which controls how much a short sequence can be stretched. For example, a sequence of length 40, when upsampled with a factor of 20, results in a sequence of length 800. The pretraining datasets are detailed in Table. 9.

C.2. Evaluation Datasets

LTSF . For evaluation, we use the standard long-horizon forecasting benchmarks: ETTm1, ETTm2, ETTh1, ETTh2, Weather, Electricity, and Traffic. We follow the same train/validation/test splits (0.6-0.2-0.2 for ETT and 0.7-0.1-0.2 for the remaining) and preprocessing protocols as in previous works (Wu et al., 2021; Zhou et al., 2021; Liu et al., 2023), including the standard scaling, which is applied independently to each channel. All the reported results represent the evaluation on the test set only. The datasets and their properties are given in Table 10.

GIFT-Eval is a benchmark designed to evaluate the generalization ability of time series forecasting models across highly diverse and heterogeneous datasets. Unlike domain-specific benchmarks, it aggregates time series from a wide range of sources—including energy, finance, healthcare, traffic, and climate—covering different sampling rates, lengths, and dynamics. The goal is to test whether models trained in a universal or foundation-style setting can transfer effectively to unseen distributions without task-specific fine-tuning. By emphasizing cross-domain robustness, scalability, and zero-shot forecasting performance, GIFT-Eval serves as a more realistic and challenging measure of a model’s ability to act as a general-purpose time series forecaster. A complete description of all the datasets is given in 11.

Table 11. Individual statistics of GIFT-Eval benchmark across all datasets as given in (Aksu et al., 2024).

Dataset	Source	Domain	Sampling Rate.	#Channels	Channels Length			#Obs	Target	Short-term		Med-term		Long-term	
					Avg	Min	Max			Var	Len	Win	Len	Win	Len
Jena Weather	(Zhou et al., 2021)	Nature	10min	1	52,704	52,704	52,704	52,704	21	48	20	480	11	720	8
Jena Weather	(Zhou et al., 2021)	Nature	hourly	1	8,784	8,784	8,784	8,784	21	48	19	480	2	720	2
Jena Weather	(Zhou et al., 2021)	Nature	daily	1	366	366	366	366	21	30	2	-	-	-	-
BizTObS - App	(Palaskar et al., 2024)	Web/CloudOps	10sec	1	8,834	8,834	8,834	8,834	2	60	15	600	2	900	1
BizTObS - Service	(Palaskar et al., 2024)	Web/CloudOps	10sec	21	8,835	8,835	8,835	185,535	2	60	15	600	2	900	1
BizTObS - L2C	(Palaskar et al., 2024)	Web/CloudOps	5min	1	31,968	31,968	31,968	31,968	7	48	20	480	7	720	5
BizTObS - L2C	(Palaskar et al., 2024)	Web/CloudOps	hourly	1	2,664	2,664	2,664	2,664	7	48	6	480	1	720	1
Bitbrains - Fast	(Shen et al., 2015)	Web/CloudOps	5min	1,250	8,640	8,640	8,640	10,800,000	2	48	18	480	2	720	2
Bitbrains - Fast	(Shen et al., 2015)	Web/CloudOps	hourly	1,250	721	721	721	901,250	2	48	2	-	-	-	-
Bitbrains - md	(Shen et al., 2015)	Web/CloudOps	5min	500	8,640	8,640	8,640	4,320,000	2	48	18	480	2	720	2
Bitbrains - md	(Shen et al., 2015)	Web/CloudOps	hourly	500	720	720	720	360,000	2	48	2	-	-	-	-
Restaurant	(Aksu et al., 2024)	Sales	daily	807	358	67	478	289,303	1	30	1	-	-	-	-
ETT1	(Zhou et al., 2021)	Energy	15min	1	69,680	69,680	69,680	69,680	7	48	20	480	15	720	10
ETT1	(Zhou et al., 2021)	Energy	hourly	1	17,420	17,420	17,420	17,420	7	48	20	480	4	720	3
ETT1	(Zhou et al., 2021)	Energy	daily	1	725	725	725	725	7	30	3	-	-	-	-
ETT1	(Zhou et al., 2021)	Energy	weekly-THU	1	103	103	103	103	7	8	2	-	-	-	-
ETT2	(Zhou et al., 2021)	Energy	15min	1	69,680	69,680	69,680	69,680	7	48	20	480	15	720	10
ETT2	(Zhou et al., 2021)	Energy	hourly	1	17,420	17,420	17,420	17,420	7	48	20	480	4	720	3
ETT2	(Zhou et al., 2021)	Energy	daily	1	725	725	725	725	7	30	3	-	-	-	-
ETT2	(Zhou et al., 2021)	Energy	weekly-THU	1	103	103	103	103	7	8	2	-	-	-	-
Loop Seattle	(Wang et al., 2023)	Transport	5min	323	105,120	105,120	105,120	33,953,760	1	48	20	480	20	720	15
Loop Seattle	(Wang et al., 2023)	Transport	hourly	323	8,760	8,760	8,760	2,829,480	1	48	19	480	2	720	2
Loop Seattle	(Wang et al., 2023)	Transport	daily	323	365	365	365	117,895	1	30	2	-	-	-	-
SZ-Taxi	(Wang et al., 2023)	Transport	15min	156	2,976	2,976	2,976	464,256	1	48	7	480	1	720	1
SZ-Taxi	(Wang et al., 2023)	Transport	hourly	156	744	744	744	116,064	1	48	2	-	-	-	-
M_DENSE	(Wang et al., 2023)	Transport	hourly	30	17,520	17,520	17,520	525,600	1	48	20	480	4	720	3
M_DENSE	(Wang et al., 2023)	Transport	daily	30	730	730	730	21,900	1	30	3	-	-	-	-
Solar	(Lai et al., 2018)	Energy	10min	137	52,560	52,560	52,560	7,200,720	1	48	20	480	11	720	8
Solar	(Lai et al., 2018)	Energy	hourly	137	8,760	8,760	8,760	1,200,120	1	48	19	480	2	720	2
Solar	(Lai et al., 2018)	Energy	daily	137	365	365	365	50,005	1	30	2	-	-	-	-
Solar	(Lai et al., 2018)	Energy	weekly-FRI	137	52	52	52	7,124	1	8	1	-	-	-	-
Hierarchical Sales	(Mancuso et al., 2021)	Sales	daily	118	1,825	1,825	1,825	215,350	1	30	7	-	-	-	-
Hierarchical Sales	(Mancuso et al., 2021)	Sales	weekly-WED	118	260	260	260	30,680	1	8	4	-	-	-	-
M4 Yearly	(Godahewa et al., 2021)	Econ/Fin	yearly-DEC	22,974	37	19	284	845,109	1	6	1	-	-	-	-
M4 Quarterly	(Godahewa et al., 2021)	Econ/Fin	quarterly-DEC	24,000	100	24	874	2,406,108	1	8	1	-	-	-	-
M4 Monthly	(Godahewa et al., 2021)	Econ/Fin	monthly	48,000	234	60	2,812	11,246,411	1	18	1	-	-	-	-
M4 Weekly	(Godahewa et al., 2021)	Econ/Fin	weekly-SUN	359	1,035	93	2,610	371,579	1	13	1	-	-	-	-
M4 Daily	(Godahewa et al., 2021)	Econ/Fin	daily	4,227	2,371	107	9,933	10,023,836	1	14	1	-	-	-	-
M4 Hourly	(Godahewa et al., 2021)	Econ/Fin	hourly	414	902	748	1,008	373,372	1	48	2	-	-	-	-
Hospital	(Godahewa et al., 2021)	Healthcare	monthly	767	84	84	84	64,428	1	12	1	-	-	-	-
COVID Deaths	(Godahewa et al., 2021)	Healthcare	daily	266	212	212	212	56,392	1	30	1	-	-	-	-
US Births	(Godahewa et al., 2021)	Healthcare	daily	1	7,305	7,305	7,305	7,305	1	30	20	-	-	-	-
US Births	(Godahewa et al., 2021)	Healthcare	weekly-TUE	1	1,043	1,043	1,043	1,043	1	8	14	-	-	-	-
US Births	(Godahewa et al., 2021)	Healthcare	monthly	1	240	240	240	240	1	12	2	-	-	-	-
Saugen	(Godahewa et al., 2021)	Nature	daily	1	23,741	23,741	23,741	23,741	1	30	20	-	-	-	-
Saugen	(Godahewa et al., 2021)	Nature	weekly-THU	1	3,391	3,391	3,391	3,391	1	8	20	-	-	-	-
Saugen	(Godahewa et al., 2021)	Nature	monthly	1	780	780	780	780	1	12	7	-	-	-	-
Temp_Rain	(Godahewa et al., 2021)	Nature	daily	32,072	725	725	725	780	1	30	3	-	-	-	-
KDD Cup 2018	(Godahewa et al., 2021)	Nature	hourly	270	10,898	9,504	10,920	2,942,364	1	48	20	480	2	720	2
KDD Cup 2018	(Godahewa et al., 2021)	Nature	daily	270	455	396	455	122,791	1	30	2	-	-	-	-
Car Parts	(Godahewa et al., 2021)	Sales	monthly	2,674	51	51	51	136,374	1	12	1	-	-	-	-
Electricity	(Asuncion et al., 2007)	Energy	15min	370	140,256	140,256	140,256	51,894,720	1	48	20	480	20	720	20
Electricity	(Asuncion et al., 2007)	Energy	hourly	370	35,064	35,064	35,064	12,973,680	1	48	20	480	8	720	5
Electricity	(Asuncion et al., 2007)	Energy	daily	370	1,461	1,461	1,461	540,370	1	30	5	-	-	-	-
Electricity	(Asuncion et al., 2007)	Energy	weekly-FRI	370	208	208	208	76,960	1	8	3	-	-	-	-

C.3. Dataset Training Details

To prevent large datasets from dominating the training process, we limit the number of training examples per dataset to 100,000, with a total dataset limit of 1,000,000 examples, which translates to $1,000,000 \times (512 + 96)$ time-points (512 and 96 represent the lookback and horizon for training, respectively for a signal example). We also employ a uniform frequency sampling strategy: datasets are categorized by their dominant frequency (e.g., the Births dataset has a dominant frequency of $\frac{1}{7}$, corresponding to daily/weekly periodicity). This frequency label guides the resampling process to match the desired frequencies. To determine the frequency of each dataset, we use the sampling rate and a manual spectrum analysis, the analyzed frequencies are also detailed in Table 9.

Common Frequencies In this work, we select multiple frequencies corresponding to natural sampling rates and train a separate linear layer expert for each one, forming the Super-Linear model. The chosen frequencies and their respective sampling rates are illustrated in Figure 12.

During training, we uniformly sample from the pool of target frequencies (see Appendix C.3), independently of the dataset source. This reflects our focus on frequency diversity rather than dataset diversity. For each dataset, we use the first 80% of its timeline for training and reserve the remaining 20% for validation. Since datasets vary in channel dimensionality and length, we adopt channel-independent (i.e., univariate) training, treating each channel as a separate time series.

Sampling Rates and Their Frequency Ratios

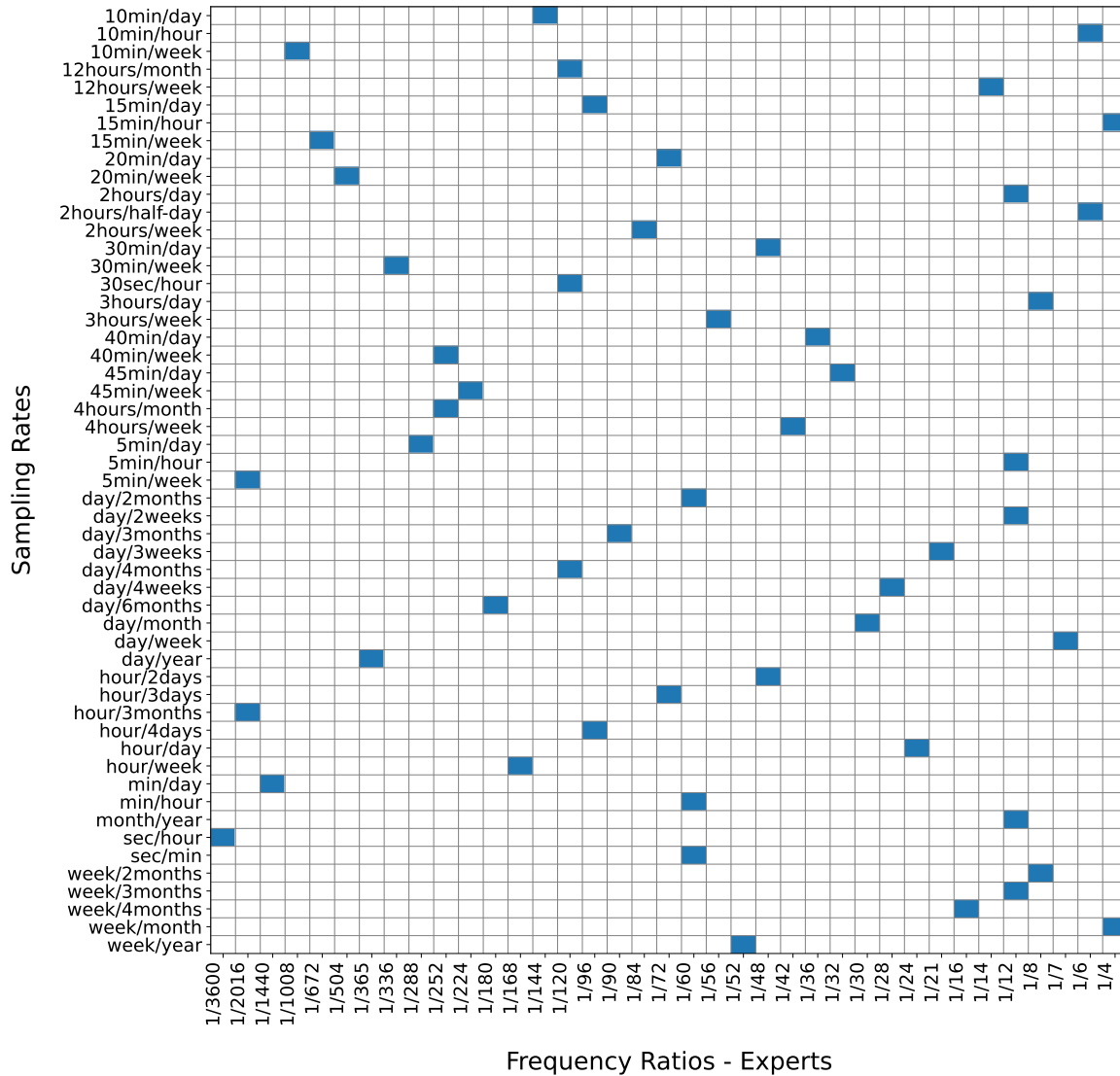


Figure 12. The common frequencies utilized by Super-Linear and their corresponding sampling rates. Each frequency expert in Super-Linear is learned with a frequency depicted in this figure, and each frequency is associated with one or more natural sampling rates.

D. Benchmark Models

D.1. Pretrained Models

Timer-XL (Liu et al., 2024c) is a decoder-only Transformer that models multivariate time series as flattened sequences of patch tokens, enabling causal next-token prediction across both time and variables. Its core component, TimeAttention, uses a Kronecker product of temporal and variable masks to enforce causal structure and capture inter-variable dependencies, while maintaining permutation-equivalence over input variables.

Time-MoE (Shi et al., 2024) is a decoder-only Transformer architecture for time series forecasting that introduces sparse mixture-of-experts (MoE) layers to scale model capacity while maintaining efficiency, dynamically activating only a subset of expert networks per input token. It employs point-wise tokenization for flexible sequence handling, rotary positional embeddings for better extrapolation, and a multi-resolution forecasting head to support arbitrary forecast horizons.

Moirai (Woo et al., 2024) is a masked encoder-based Transformer designed for universal time series forecasting, featuring multi-patch size input/output projections to handle multiple sampling frequencies and Any-variate Attention to flexibly model arbitrary multivariate sequences. It outputs parameters for a flexible mixture of parametric distributions, enabling probabilistic forecasting across diverse domains, variate dimensionalities, and data distributions.

TimesFM (Das et al., 2024) model is a decoder-only Transformer architecture for time-series forecasting that uses input patching to efficiently represent and process long sequences, inspired by tokenization in language models. It is pretrained on a large and diverse corpus of real and synthetic time-series data, enabling accurate zero-shot forecasts across different domains, time granularities, and forecast horizons.

Chronos (Ansari et al., 2024) is an adaptation of language models for time series forecasting, where time series data is tokenized through scaling and quantization into discrete bins, allowing standard language models to be used for probabilistic forecasting. It trains models on a large set of time series, using data augmentation techniques like TSMixup and KernelSynth, and performs zero-shot forecasting without the need for task-specific adjustments or architecture changes.

ROSE (Wang et al.) a lightweight general time series forecasting model designed for multi-domain data. Unlike other foundation models that mainly rely on scaling datasets and model sizes, ROSE tackles two key challenges: learning unified representations across heterogeneous domains and enabling adaptive transfer to domain-specific tasks. To achieve this, the authors propose Decomposed Frequency Learning, which disentangles complex temporal patterns by applying frequency-based masking and reconstruction, leading to generalized representations, and the Time Series Register (TS-Register), which stores domain-specific representations during pre-training and adaptively selects relevant ones for downstream tasks via fine-tuning with low-rank updates.

TTM (Ekambaram et al., 2024) Multi-level Tiny Time Mixers are lightweight pre-trained models for multivariate time-series forecasting, designed to rival or outperform large foundation models while using only 1M parameters. Built on the efficient TSMixer architecture, TTM replaces costly Transformer self-attention with MLP-Mixer blocks and gated attention, enabling fast pre-training and inference. To handle heterogeneous, multi-resolution datasets, TTM introduces adaptive patching (AP), diverse resolution sampling (DRS), and resolution prefix tuning (RPT), which improve robustness across domains and temporal scales. Its multi-level modeling strategy first pre-trains channel-independent representations, then fine-tunes with channel mixing to capture correlations across targets and exogenous signals—capabilities often missing in larger models.

Sundial (Liu et al., 2025) is a family of scalable time series foundation models that directly model continuous sequences using TimeFlow Loss, a flow-matching objective that enables Transformers to generate multiple probable forecasts without discrete tokenization or parametric densities. With minimal Transformer adaptations and pre-training on TimeBench (a trillion time points), Sundial achieves state-of-the-art zero-shot results on major benchmarks while delivering fast, flexible, and reliable generative forecasting.

VisionTS (Chen et al., 2024) repurposes a pre-trained visual masked autoencoder (MAE) for time series forecasting by converting time series into images and framing forecasting as masked patch reconstruction. This simple reformulation enables strong zero-shot performance and near state-of-the-art results with minimal fine-tuning, showing visual models can serve as effective foundation models for time series.

D.2. In-Domain Models

UniTST (Liu et al., 2024a) model employs a unified attention mechanism that simultaneously captures both inter-variate and intra-variate dependencies by flattening patches from different variates into a unified sequence. To reduce memory complexity, it introduces a dispatcher mechanism, which aggregates dependencies across tokens and distributes the information efficiently, ensuring effective modeling of time-series data with large variates.

CycleNet (Lin et al., 2024a) is designed to explicitly model periodic patterns in time series data using the Residual Cycle Forecasting (RCF) technique, which leverages learnable recurrent cycles to capture inherent cyclic components. The model then predicts the residual components of the cycles using a simple backbone, either a linear or shallow MLP model, providing an efficient and powerful solution for long-term time series forecasting.

iTransformer (Liu et al., 2023) model design independently embeds each time series as a variate token, applying self-attention to capture multivariate correlations between these tokens. The model then utilizes feed-forward networks to learn series representations, eliminating the need for complex encoder-decoder architectures while improving efficiency and forecasting accuracy.

TimesNet, (Wu et al., 2022) a deep learning framework designed to capture intricate temporal variations in time series data by leveraging the multi-periodicity inherent in real-world time series. It introduces several key innovations and methods for better handling complex temporal patterns, such as intraperiod-variation (short-term variations within a period) and interperiod-variation (long-term variations between different periods).

PatchTST (Nie et al., 2023) is a Transformer-based architecture designed for multivariate time series forecasting, incorporating two key innovations: patching and channel-independence. Patching divides time series into non-overlapping subseries to capture local semantic information, while channel-independence processes each univariate time series independently to reduce computational complexity and enhance forecasting accuracy.

Autoformer (Wu et al., 2021) is a time series forecasting model that incorporates a decomposition architecture to handle long-term temporal patterns. It introduces an Auto-Correlation mechanism that efficiently discovers period-based dependencies and aggregates similar sub-series, significantly improving both information utilization and computational efficiency for long-term forecasting.

FreqMoE (Liu, 2025) integrates a Frequency Decomposition Mixture-of-Experts (MoE) module, where expert networks focus on distinct frequency bands of the time series data, with a gating network dynamically adjusting the contribution of each expert based on the frequency magnitude. The model then utilizes residual-connected frequency domain prediction blocks to iteratively refine predictions, effectively capturing complex temporal and frequency patterns for accurate time series forecasting.

MoLE, (Ni et al., 2024) The Mixture-of-Linear-Experts model augments linear-centric time series forecasting models by training multiple linear models (experts) and a router model that adaptively mixes their outputs based on temporal patterns. Using an embedding of the first timestamp, the router assigns weights to each expert, allowing them to specialize in different temporal periods, thus improving forecasting accuracy while maintaining the simplicity of linear models.

MTLinear (Nochumsohn et al., 2021) for multivariate time series forecasting groups similar variates based on their Pearson Correlation Coefficient, assigning each group a separate linear module. This design leverages multi-task learning principles to address gradient conflicts and balance the contribution of variates during training, improving forecasting accuracy and efficiency.

DLinear, (Zeng et al., 2023) a linear based model that first decomposes the input time series into trend and seasonal components using a moving average kernel. It then applies separate one-layer linear models to each component and combines their outputs to make the final prediction.

E. Super-Linear Frequency Expert Weights

As shown in Figure 13, the frequency experts capture distinct, well-defined patterns associated with the corresponding periodic lag. In addition, the complementary experts reveal additional structure that the model did not learn during stage 1 training. For example, `comp_11` and `comp_8` exhibit activations similar to those of the frequency experts, suggesting they encode complementary frequency information. In contrast, experts such as `comp_0` and `comp_5` display more arbitrary behavior, which appears to compensate for patterns that the frequency experts may struggle to extract.

F. Hyperparameters

In this section we present the hyper parameter for the pretrained ZS Super-Linear 12 and in-domain (FS) 13.

Table 12. Description of hyperparameters for pretrained (ZS) Super-Linear configuration.

Hyperparameter	Description	Values
Learning Rate	Controls the step size in gradient descent	0.1
Batch Size	Number of training examples used in one iteration	512
Channel Organization	Processing input data as either univariate (channel independent) or multivariate during training	Channel Independent
Number of Epochs	Number of times the entire dataset is passed through the model	30
Patience	Number of epochs without improvement before early stopping	5
Learning Rate Adjustment (decay)	Strategy for adapting the learning rate during training	$0.9^{epoch-3}$ if $epoch > 3$ else 1
Top-k Experts	Number of selected experts in training	12
Dataset Max Size	Maximum number of samples considered for training from each dataset	100,000
Frequency Experts N_f	Number of different frequency experts	37
Complementary Experts N_c	Additional experts used alongside the frequency ones	12
Optimizer	Algorithm used for model parameter optimization	Adam
Gate Weight Dimension M	Dimension proportional to spectrum length	2,500
Lookback	Number of past timesteps used as input for prediction	512
Forecast Horizon	Future timesteps predicted by the model during training only	96
Gate Noise Std	Standard deviation of noise added to gating mechanism	0.1
Maximal Energy Loss $E_{maxloss}$	The maximum allowed fraction of normalized energy loss during the resampling process	0.2
Scales $S = \{s_1, s_2, \dots\}$	The resampling scale factor for the interpolation of the <i>Long Lookback Resample Search Algorithm</i>	{2, 4, 6}
Energy Loss Penalty Scaler λ	A scaler to control the incurred energy loss penalty of the <i>Long Lookback Resample Search Algorithm</i>	2

Table 13. Description of hyperparameters for in-domain (FS) Super-Linear configuration.

Hyperparameter	Description	Values
Learning Rate	Controls the step size in gradient descent	0.05
Batch Size	Number of training examples used in one iteration	32
Channel Organization	Processing input data as either univariate (channel independent) or multivariate during training	Multivariate
Number of Epochs	Number of times the entire dataset is passed through the model	30
Patience	Number of epochs without improvement before early stopping	5
Learning Rate Adjustment (decay)	Strategy for adapting the learning rate during training	none
Top-k Experts	Number of selected experts in training	6, 8, 10, 12, 20
Dataset Max Size	Maximum number of samples considered for training from each dataset	none
Frequency Experts N_f	Number of different frequency experts	37
Complementary Experts N_c	Additional experts used alongside the frequency ones	10
Optimizer	Algorithm used for model parameter optimization	Adam
Gate Weight Dimension M	Dimension proportional to spectrum length	2,500
Lookback	Number of past timesteps used as input for prediction	512
Forecast Horizon	Future timesteps predicted by the model during training only	96
Gate Noise Std	Standard deviation of noise added to gating mechanism	0.1

G. Limitations

Despite its efficiency and strong performance, Super-Linear has several limitations. First, its reliance on linear representations may restrict its ability to capture complex temporal dependencies or nonlinear patterns that are common in many real-world time series. While the frequency-specialized design helps mitigate this to some extent, it may still fall short in scenarios where nonlinear interactions between frequencies are crucial. Second, although Super-Linear can process relatively long input sequences due to its lightweight architecture, its context modeling is limited by 512 lookback steps, which may hinder performance on tasks that require reasoning over very long lookback contexts. Finally, the model may struggle with time series that exhibit uncommon or transient frequency components not well-aligned with the predefined frequencies in 12. Expert specialization relies on fixed frequency filters, which may struggle to represent rare or shifting frequency patterns, potentially hindering generalization in such scenarios. While complementary layers aim to bridge information gaps—particularly for uncommon frequencies—this limitation may still persist.

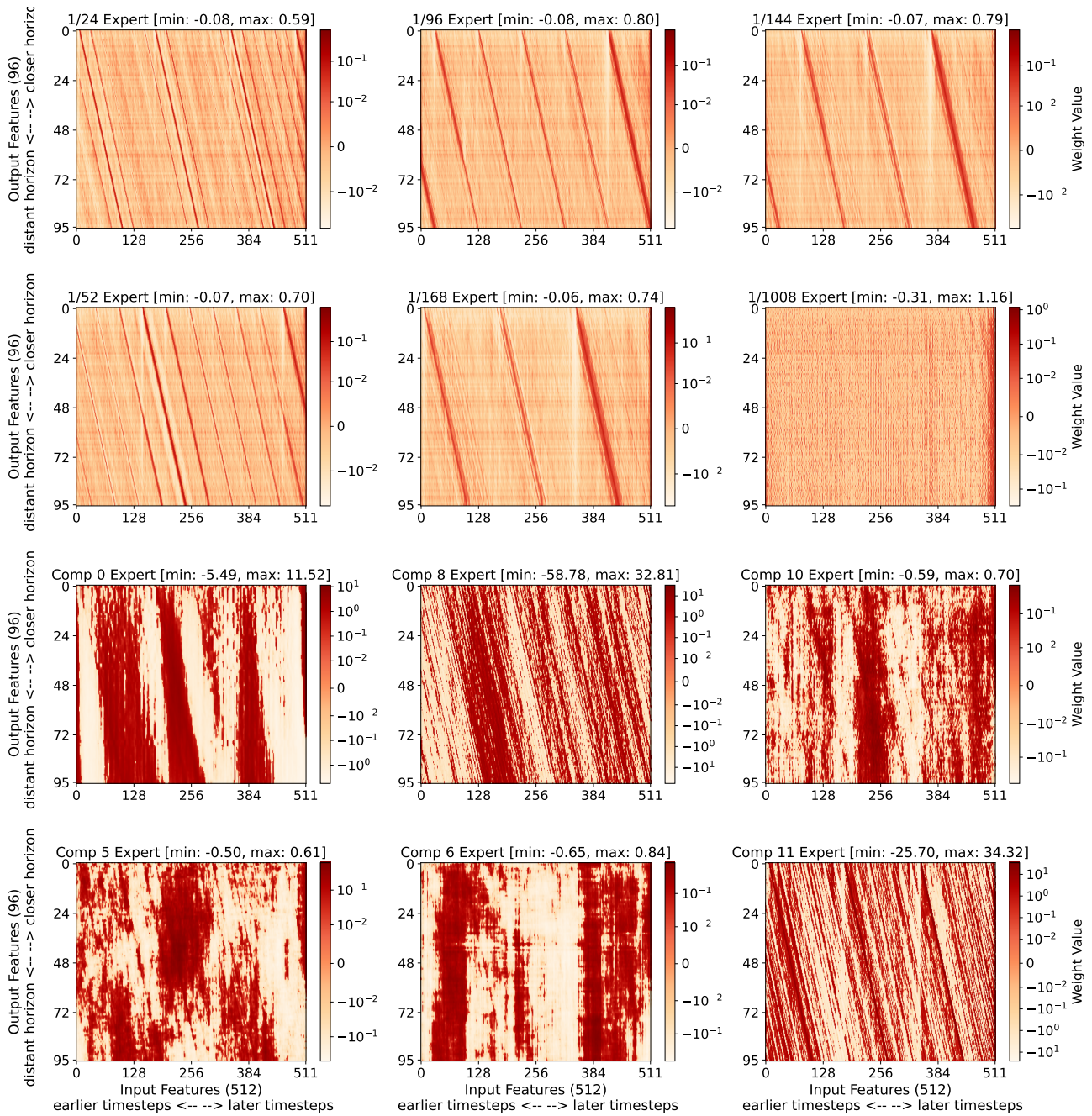


Figure 13. Visualization of the Super-Linear frequency and complementary expert weights.